Applied Geochemistry 196 (2026) 106646

Contents lists available at ScienceDirect

Applied Geochemistry

journal homepage: www.elsevier.com/locate/apgeochem

THEREDA: Thermodynamic reference database for geochemical modelling of nuclear waste disposal under saline conditions – Application, overview, and new developments

Helge C. Moog [a,*], Marcus Altmaier [b], Frank Bok [c], Vinzenz Brendler [c], Daniela Freyer [d,**], Xavier Gaona [b], Sven Hagemann [a], Claudia Joseph [e], George-Dan Miron [f], Melanie Pannach [d], Julia Sohr [d], Wolfgang Voigt [d], Marie Voss [g], Laurin Wissmeier [g]

[a] Gesellschaft für Anlagen- und Reaktorsicherheit, Process Analysis Division, Braunschweig, Germany
[b] Karlsruhe Institute of Technology, Institute for Nuclear Waste Disposal, Karlsruhe, Germany
[c] Helmholtz-Zentrum Dresden-Rossendorf e.V., Institute for Resource Ecology, Dresden, Germany
[d] Technische Universität Bergakademie Freiberg, Institute of Inorganic Chemistry, Freiberg, Germany
[e] Bundesgesellschaft für Endlagerung (BGE) mbH, Eschenstraße 55, Peine, 31224, Germany
[f] Paul Scherrer Institute, Laboratory for Waste Management, Villigen, Switzerland
[g] CSD Engineers AG, Groundwater Modelling and Safety Analyses, Aarau, Switzerland

ARTICLE INFO

Editorial handling by Dr Dmitrii A. Kulik

Keywords:
Thermodynamic database
Nuclear waste management
Radionuclides
Oceanic salts
Heavy metals
Pitzer approach
Cement systems
Brines
Solubility
Speciation
Solid-liquid phase equilibria

ABSTRACT

The Thermodynamic Reference Database (THEREDA) is designed for geochemical calculations in the context of repositories for radioactive waste under high-saline conditions. For this purpose, it adopts the Pitzer ion-interaction approach. THEREDA is currently the only database worldwide that allows comprehensive poly-thermal calculations (up to at least 100 °C) of the hexary system of the oceanic salts Na-K-Mg-Ca-Cl-SO_4-H_2O, including acids, bases, and CO_2/carbonates. Its validity is documented primarily, yet not exclusively, by application to solubility data. THEREDA's potential to predict the development of the geochemical environment, e.g. in the event of an intrusion of solution, constitutes a prerequisite for the engineering design of a nuclear waste repository with regard to the selection and placement of plug and sealing system components.

The focus of THEREDA lies on the calculation of solubilities of radionuclides (actinides, fission and activation products), chemotoxic and matrix elements e.g., canister materials, and compounds having an impact on the overall geochemical milieu in the near field of a repository under high-saline conditions.

Special features of THEREDA besides its focus on high-saline solutions are procedures for testing prior to any release combined with intercode-comparison, extensive and publicly available validation against published experimental data, and systematic application of a scheme to mark data with regard to quality, reliability, and origin. Traceability of data and validated experimental results to published sources is also emphasised. This documentation is in part realised in ready-to-use parameter files for users, and in part on the website (www.thereda.de). Another feature is the possibility for operation of THEREDA by several institutions in a networked manner.

To highlight THEREDA's potential, examples for applications of the database are given. Additionally, ongoing efforts for the further development of THEREDA are described in the outlook at the end of this article.

1. Introduction

Performance assessment for the disposal of nuclear waste in deep geological formations is supported by an estimate on how the near field (containment, backfill) as well as the far field (host rock, cap rock) will evolve geochemically. This geochemical evolution is mainly associated

* Corresponding author. Gesellschaft für Anlagen- und Reaktorsicherheit gGmbH, Process analysis division, Theodor-Heuss-Strasse 4, 38122, Braunschweig, Germany.
** Corresponding author. Technische Universität Bergakademie Freiberg, Institute of Inorganic Chemistry, Leipziger Str. 29, 09599 Freiberg, Germany.
E-mail addresses: Helge.Moog@grs.de (H.C. Moog), daniela.freyer@chemie.tu-freiberg.de (D. Freyer).

https://doi.org/10.1016/j.apgeochem.2025.106646
Received 28 July 2025; Received in revised form 30 October 2025; Accepted 27 November 2025
Available online 29 November 2025

with the intrusion of aqueous solutions.

Three options of host rock are investigated worldwide: rock salt, argillaceous or plastic clay, and crystalline rock (granite/granodiorite/gneiss). In Germany, this selection has been codified by law (StandAG, 2023). The term "rock salt" usually refers to evaporites deposited upon the past evaporation of sea water. While this term is sometimes used as a synonym for the main component NaCl (halite), rock salt is actually composed of a succession of several mineral phases which reflects seawater composition and temperature at the time of precipitation, and which contains the entire system of oceanic salts. The general notation Na-K-Mg-Ca-Cl-SO_4-H_2O for the six-component system includes all aqueous species that can be formed by dissociation reactions/protolysis equilibria with water. In the case of the extension by carbonate, accordingly, these are the species CO_2, HCO_3^-, and CO_3^{2-}.

Depending on the host rock, an intrusion of aqueous solution into the near field can be regarded as probable or as a highly improbable event in the evolution of a repository. The host rock also has a crucial impact on the ionic strength of these solutions.

In the event of aqueous solution accessing the near field, performance assessment is mainly aimed at assessing the maximum likely mass stream of radionuclides or other contaminants exiting the near field. This serves as the "source term" in integrated codes in which their migration through overburden layers of rock and – ultimately – their potential entry into the biosphere is modelled. Throughout the complete migration path, the mobility of contaminants is subject to chemical processes such as dissolution/precipitation or desorption/sorption. These processes can be assessed using codes for geochemical modelling.

The hypothetical release of contaminants from the near field can be broken down into a sequence of certain processes which are linked to the temporal evolution following the access of aqueous solution, i.e.

- Dissolution/precipitation occurring when aqueous solution reacts with the host rock while approaching the near field;
- Interaction with buffer and backfill materials, including plugs and seals;
- Corrosion of waste containments;
- Mobilisation of contaminants from the waste matrix;
- Interaction of mobilised contaminants with corrosion products from the waste containment;
- Interaction of contaminants with (corroded) buffer and backfill materials;
- Interactions of contaminants with the host rock.

To assess the above-mentioned processes, geochemical model calculations are performed, which in most cases assume local thermodynamic equilibrium. Numerous codes were developed for these calculations in the past decades, some of which were abandoned.

These codes need thermodynamic data in a code-specific format, usually extracted from a larger thermodynamic database. The term "thermodynamic data" in the present context refers to equilibrium constants or free enthalpies of formation, depending on the type of geochemical code used.

When considering heat-emitting radioactive waste, such a thermodynamic database needs to take the temperature dependence of reactions into account. This is reflected in standard molal enthalpies of reactions, standard molal entropies of reactions and standard (or partial) molal heat capacities of reactions. In many cases, however, these quantities are only known in aggregated form as temperature-dependent equilibrium constants.

For now over about 35 years the OECD Nuclear Energy Agency (NEA) pursues the goal of developing an internally consistent thermochemical database (hereafter referred to as "NEA-TDB"). These efforts condensed into 15 published volumes containing selected thermodynamic data for a vast number of compounds. The volumes are the result of the work of teams of experts who evaluated and critically reviewed published primary experimental data. Review processes followed predefined guidelines for quality, data-deduction and the assessment of uncertainties. The NEA-TDB project is still ongoing. A comprehensive account on the project was given by Ragoussi and Costa (2019).

However, even though the NEA-TDB developed into an international standard for high-quality thermodynamic data and is as such highly acclaimed in the scientific community, it is not being developed for the specific requirements of geochemical modelling for the near and far field of nuclear waste repositories. This is in part due to missing data for solid phases and aqueous species that are essential for modelling purposes but for which no thermodynamic data that meet the high-quality standards of the NEA-TDB can be derived. But due to its general validity at zero ionic strength and the vast effort already exerted by experts, it is used as foundation in national database projects and extended or modified to meet the demands of geochemical calculations in the context of national nuclear waste disposal applications and specific host rocks.

If crystalline rock (e. g. Finland, Sweden, Czech Republic) or clay stone (e. g. France, Belgium, Switzerland) are intended to serve as host rock, aqueous solutions are anticipated to have a low ionic strength in most cases, with some exceptions like sedimentary bedrocks in the Canadian Shield or Cretaceous argillites in Northern Germany. Thermodynamic databases contain aqueous species and solid phases likely to occur under these conditions and no ion-specific corrections to aqueous species activity coefficients are necessary. ANDRA (France), ONDRAF-NIRAS (Belgium), and NWS (UK) joined efforts in the development of ThermoChimie (Giffaut et al., 2014; Grivé et al., 2015; Madé et al., 2025), originally promoted by ANDRA. Another example is Nagra's thermodynamic database (Switzerland), set up by the Paul Scherrer Institute (PSI) (Hummel et al., 2002; Hummel and Thoenen, 2023; Thoenen et al., 2014). Both databases are publicly available on the internet and include ion-specific corrections according to the specific ion interaction theory (SIT), see Brönsted (1922a, 1922b), Guggenheim (1966), Scatchard (1936), which expand the validity of geochemical calculations with respect to higher ionic strength (up to 3.5 mol/kgw) for some simple, binary background electrolytes such as NaCl, $NaNO_3$, or $NaClO_4$.

In other countries, host rock types of evaporitic origin are considered as candidates for nuclear waste disposal, e. g. in U.S.A. or Germany (StandAG, 2023). Aqueous solutions in these formations (hexary system of oceanic salts: Na-K-Mg-Ca-Cl-SO_4-H_2O) exhibit ionic strengths far beyond the validity limit of the extended Debye-Hückel equation or related approaches for activity coefficients (>3.5 mol/kgw) and can be saturated with up to five salt minerals. These conditions require the application of activity correction formalisms accounting for ion-specific interactions that must be suitable to cope with complex (up to hexary) systems. Another special case can arise in Northern Germany where layered rock salt is overlain by argillaceous formations, in which aqueous solutions containing Al- and Si-species are likely to react with halite and anhydrite. Aqueous solutions under these conditions, though undersaturated, can still feature an ionic strength of more than 1 mol/kg. Consideration of Si- and Al-species in high-saline solutions is covered in chapter 3.4.2.

The specific requirements posed by the geological situation in Germany were the motivation to set up a national project for the creation of a **Ther**modynamic **Re**ference **Da**tabase (THEREDA). In an earlier publication (Moog et al., 2015), THEREDA was described in technical and formal terms, only few of which have changed since 2015. Therefore, the present paper will be focused on special features of THEREDA and its recent evolution with respect to the different fields of application.

2. Special features

2.1. Validity for highly-saline to salt-saturated solutions of evaporitic minerals

For the reasons given, a thermodynamic database consistent with the extended Debye-Hückel equation for the calculation of activity

coefficients is inadequate for many of the relevant conditions in Germany. Even more so since it is required to not only predict contaminants' solubility but also to model the mineral paragenesis and solution composition in the saturated, hexary system of oceanic salts (details to this aspect of the development of THEREDA s. Chapter 3.1.1). Consequently, several institutions in Germany, which have since become partners in the development of THEREDA, began to apply the Pitzer formalism in their modelling efforts early on. As of 2011, THEREDA went online as a publicly accessible thermodynamic database.

It should be noted that other projects existed or still exist in the U.S. A. to set-up Pitzer databases. Yucca Mountain, for instance, was regarded as a potential site for the disposal of high-level nuclear waste, and a specific database was set up by Sandia National Laboratories (SNL) (Moffat and Jové-Colón, 2009), distributed with the geochemical code EQ3/6 (for information about this code, see Wolery et al. (1990)). Later, the database was implemented for the code Cantera (Goodwin et al., 2015) and its development is documented in several reports and articles. Yet, there is no straightforward way to access a present state of a "Yucca Mountain thermodynamic database", only legacy parameter files for EQ3/6 are available. However, the authors of this databases declared explicitly that it was not the aim to generate a thermodynamically consistent database. It was supposed to enable the calculation of equilibria important for a waste isolation plant. It seems that the latest version named "data0.ypf.R2" was released in 2006 and was converted into a PHREEQC-format afterwards (Benbow et al., 2008). The Waste Isolation Pilot Plant (WIPP), as another example, is the only US-American disposal site in operation for defense-related radioactive waste. While the corresponding thermodynamic database does not seem to be accessible publicly, several publications indicate continuous work on it, e. g. Jang and Nemer (2016), Xiong et al. (2017), Xiong and Domski (2016).

In 2014, a multinational working group "Modelling Chemical Speciation in Seawater to Meet 21st Century Needs (MARCHEMSPEC)" was established within the Scientific Committee on Oceanic Research. It works to establish a thermodynamic database for seawater using the Pitzer formalism (Turner et al., 2016). The working group is present on the internet under https://marchemspec.org/wp/ and offers software compatible with Windows, macOS and Linux for the calculation of acid-base equilibria and inorganic complexation in seawater. Obviously, these efforts have a clearly different focus as the database is aimed at needs for oceanographic requirements (temperature 5–45 °C, below saturation limits of oceanic salts, no radionuclides, pressure up to 1′000 bar, no hyperalkaline conditions). As in the former cases, there is no straightforward way to access the thermodynamic database.

The equations of the Pitzer formalism are described in the original publication by Pitzer and co-workers, with a more recent account given in Pitzer (1991). While the Debye-Hückel equation accounts for electrostatic, non-specific, and long-range interactions between ions of opposite charge, the Pitzer equations add non-electrostatic, specific, and short-range interactions. In contrast to the SIT formalism, where only binary interactions between ions of opposite charge and between ions and neutral species are accounted for ("SIT-coefficients"), Pitzer extended his approach even further by accounting for non-electrostatic interactions with (or between) uncharged species and triple interactions between charged and/or uncharged species. Essentially, the Debye--Hückel equation is extended by a summation of terms, in which each term represents one interaction. Each term is a function of molality of interacting species multiplied with a coefficient ("Pitzer-coefficient"). Though quite bulky for ternary or quaternary solutions, when applied to experimental data, Pitzer's equations form a system of linear equations with respect to the Pitzer-coefficients, which can easily be solved using standard mathematical routines.

Generally, the activity of aqueous species is related to activity coefficients γ_i specific to certain interacting species and solute concentrations m_i. Because of the relation

$$a_i = \gamma_i m_i \tag{1-1}$$

with a_i = activity of species i, it follows from the former statement that Pitzer-coefficients in general may be obtained from all experiments in which solute concentrations m_i and solute activities a_i are measured simultaneously. Examples are the measurement of water activity (isopiestic methods or direct measurement of vapour pressure) or electromotoric force (emf). In a more intricate way, this statement is also valid for the measurement of solubility, where at some point of data processing, the solubility constant (which is an activity product for salts) is postulated at thermodynamic equilibrium.

Strictly speaking, this implies that the speciation in the system of interest is known. In highly concentrated salt solutions, this may pose a significant problem, because numerous complex species can be formed whose concentration and activity cannot be measured independently. In some cases, this obstacle can be overcome by neglecting complex species and accounting for their impact on solid phase solubilities by adaptation of Pitzer-coefficients between supposedly fully dissociated ions. This allows accurate calculations even for complex systems but leads to a less realistic representation of speciation in the solution. Accordingly, for some comparable systems, THEREDA may contain fewer species than other databases involving Debye-Hückel or SIT ionic strength corrections.

Expanding databases relying on Pitzer coefficients, like THEREDA, is more complicated than it might be for other databases, as the introduction of new chemical elements or species must consider the background of already existing Pitzer interactions for related systems (maintaining the Pitzer coefficients of binary resp. ternary subsystems). For instance, it is not sufficient to implement a published solubility constant of a mineral without an evaluation of the effect of interactions of oceanic salt ions with the ions of the mineral when it is dissolved. In most cases interaction parameters or modified speciation schemes have to be implemented.

2.2. Application examples

The most stringent test of any thermodynamic database is its ability to reproduce experimental data from peer-reviewed sources. The agreement with experimental data, which were used during the process to determine the thermodynamic data that are part of the database ("calibration data"), is trivial. However, THEREDA is continuously tested against systems which were investigated independently from the derivation of parameters ("validation data"). For the sake of transparency, calculations showing a poor agreement with experimental data are not excluded from the list of application examples.

Application examples serve three goals: first to validate THEREDA; second, to show general limitations of the model and third, to signalise to the user which systems THEREDA is NOT tested for. The third goal is due to the fact that a large database inevitably enables the user to apply it to systems for which no experimental data are available. However, the user should be aware that the number of tested systems will never match the number of systems that can be reliably modelled with THEREDA. Conversely, application of THEREDA to any system which is not part of the application examples, should be regarded with caution.

The list of application examples is accessible on the homepage of THEREDA (www.thereda.de). System compositions can be selected and composed elementwise leading the user to references for complex systems. Each application example is depicted by a diagram and accompanied by references the experimental data were taken from. Wherever possible, references are supplied with DOI.

Maintenance and extension of application examples is an ongoing activity of the THEREDA project. As of writing this paper, almost 600 application examples are available to the user.

2.3. Test calculations

Any thermodynamic database represents a complex system of independent ("entered") and dependent ("internally calculated") thermodynamic data. It should be noted that along with this data, phase constituents selected for all phases (aqueous, gaseous, all solid phases) are an important part of the thermodynamic model. For example, even with otherwise identical thermodynamic data, removal or addition of a single aqueous species can lead to significantly different computational results.

THEREDA is being worked on by several independent partners editing the database using a web-based graphical user interface. While extensions and modifications of THEREDA are communicated internally it cannot be excluded altogether that data manipulations intended for the improvement in one system yield adverse side effects in another one. For example, the addition of nitrate cannot be done by simply adopting Pitzer coefficients and solubility constants from published papers. Pitzer coefficients and solubility constants optimised for the ternary system NaCl-$NaNO_3$-H_2O at 25 °C, for instance, cannot be adopted in a straightforward way because they are correlated and form an internally consistent set of data. When all solubility constants and Pitzer coefficients related to the NaCl-H_2O subsystem are already fixed by earlier optimization steps, including yet other subsystems, experimental data for the ternary system NaCl-$NaNO_3$-H_2O must be refitted while retaining Pitzer coefficients and the solubility constant for halite (binary system NaCl-H_2O). Another example is the subsequent addition of an aqueous species, for example $Ca(OH)^+$, present in Cemdata18, which is a database for the stability of Portland cements and alkali-activated materials in low-saline solutions without the need for Pitzer coefficients (Lothenbach et al., 2019). This addition would be detrimental for the results for alkaline Ca-containing systems in high-saline solutions, where the complete set of solubility constants and Pitzer coefficients was optimised without consideration of this additional species.

To ensure that newly released versions of THEREDA remain valid for geochemical systems that earlier releases were developed for, an increasing number of test calculations is performed with all supported codes prior to any release. Note, the difference between "application examples" (see section 2.2) and "test calculations": while the former serve to demonstrate the capability (or limits) of THEREDA to reproduce experimental data, the latter serve to probe the database for errors which might have occurred during data capture, internal calculation, and code-specific export. Any test calculation creates one or more pairs of datatype and value. To minimise the effort, any test calculation is designed to check the highest possible number of thermodynamic data points or Pitzer coefficients. Any extension to THEREDA is accompanied by considerations as to which additional test calculations are necessary to check it. When a new release enters the test phase, the results of all test calculations are compared with the results of all earlier releases. If significant differences occur the respective systems with their concomitant thermodynamic data and Pitzer coefficients are inspected.

Due to different capabilities of the supported codes (see chapter 4.1), not all test cases can be run by all codes. But for the vast majority of test calculations, no problems occur and thus test calculations offer an intercode comparison to ensure that THEREDA produces the same results for the same system using different codes.

2.4. Traceability

To contribute to the overall credibility of statements on dissolution and crystallisation processes and, therefore, on the solubility of hazardous contaminants in the near field of a repository for radioactive waste, THEREDA strives to link all selected data to publications that are available to the public. This information is not only provided in reports but also in the code-specific parameter files for the user. This commitment also extends to experimental data in application examples (see chapter 2.2), where references are provided. Lastly, references are also provided in a subsection of the THEREDA homepage, where thermodynamic data and Pitzer coefficients can be looked up and downloaded. As of writing this paper, more than 1′000 references are saved in THEREDA.

2.5. Quality, reliability, and origin of data

Geochemical calculations required in the context of repositories for nuclear waste disposal must cover chemical elements, materials, and boundary conditions of relevance in the near and far field of a repository. About 50 chemical elements need to be considered altogether, not all of which need to be modelled using the Pitzer formalism, as some decay products form rather late, when their parent nuclides have already migrated beyond the zone where high-saline conditions prevail.

Yet, the sheer number of about 50 chemical elements indicates that setting up an internally consistent thermodynamic database is a formidable task, and it is likely – especially considering the large time scales on which the safety assessment of nuclear waste repositories must be provided – that the quality of thermodynamic data will vary: for some closely investigated systems the quality of related data may be excellent and geochemical predictions might be reliable; for other systems, however, experimental data may be scarce or even non-existent, and estimations become necessary.

For the documentation of the overall reliability of data and to facilitate future decisions as to its further development, a simple system for the categorisation of data was established for THEREDA, which is part of the code-specific parameter files issued to the user. Thermodynamic data are categorised in terms of their overall quality, and how they were determined. A third categorisation scheme is applied to the references. All schemes are built up of integer numbers.

The scheme for the overall quality of data (Table 1) includes rank "0", which is applied, for example, to enthalpies of formation of chemical elements at 25 °C in their standard state (which is zero).In contrast, rank "3" is assigned to questionable data and used only if the omission of said data would lead to unreasonable computational results. One example may be neutral metal hydroxide or carbonate complexes, which are difficult to detect and whose formation constants are assigned a high uncertainty, but which are a necessary part of the thermodynamic model to describe the overall pattern of solubility as a function of ligand concentration. This rank is also applied if the speciation is unclear or doubts about the auxiliary data exist which were used in the process of determining the datum. Rank "2", as opposed to rank "1", signifies data which are reliable within the given range of error, but where the error is relatively high (because of experimental problems, errors in utilized auxiliary data, or uncertainties due to inappropriate analogy data or methods of estimation).

The second scheme categorises how data were derived (Table 2). This extends to the question if data are based on formation- or reaction-related data, and it covers the question if data are based on any experiment at all. Not surprisingly, data based on experimental data receives the best scoring. Data derived from chemical analogues get the next highest ranking. One example are complex formation constants or Pitzer-coefficients of americium, which were derived from experiments with neodymium and curium. The lowest data class is assigned if neither experimental data nor chemical analogues are known, and data are based purely on estimations, such as approximative equations or correlations.

Table 1
Scheme for the quality of data in THEREDA.

Symbol	Description
0	By definition/convention fixed value
1	Recommended datum
2	Supplemental/provisional datum
3	Questionable datum

Table 2
Scheme for class and category of data in THEREDA; a combination of both is assigned to all independent data.

Data Class	
Symbol	Description
0	By definition or convention
1	Value based on experimental data
2	Chemical analogue value, based on experimental data
3	Estimated value, based on founded correlations and models
Category	**Description**
F	Value based on formation data
NA	By definition/convention fixed value
R	Value based on reaction data

Table 2 illustrates that the class of data in THEREDA is composed of two aspects: the first one ("Symbol") refers to the scoring, the second one refers to formation- and reaction-related data. For example, if a solubility constant was determined in solubility experiments, it will receive category "R" (reaction). If, in contrast, a solubility constant was derived from standard formation data, it receives category "F" (formation). Geochemical modellers are often unaware that many of the thermodynamic data they use in their models were never determined from reversible solubility equilibria. The scoring reflects the preference of experimental vs. analogue or estimated data. Like the scoring of data quality (Table 1), it aims at the quick assessment of large data sets and the prioritization of future efforts to improve the database. Furthermore, the numeric scoring facilitates the extension to the assessment of dependent data which are internally calculated.

The third categorisation scheme is applied to the references the data in THEREDA were adopted from (Table 2 and 3). It should be noted that, regardless of its scoring, public availability of the source is an indispensable prerequisite for its use in THEREDA.

3. Fields of application

3.1. Host rock salt and salt chemistry: interactions between evaporite minerals and solution

Evaporitic sediments are distributed worldwide and often form rock salt deposits that are several hundreds to thousands of meters thick. Evaporation processes over millions of years precipitated all dissolved salts from seawater with NaCl as the main component and all others such as KCl, $MgSO_4$, $MgCl_2$, etc. forming a variety of salt minerals. In addition to this classic model of seawater evaporation (Warren, 2016), the formation of large salt accumulations depending on geological formations is also explained by other models such as the hydrothermal salt model (Hovland et al., 2018) or serpentinization (Scribano et al., 2017; Debure et al., 2019).

Understanding the crystallisation, re-dissolution, and re-crystallisation processes.

(1) during the genesis of a particular geological formation,
(2) for extraction processes (e.g. potash salts, etc.),
(3) for safety analysis of a repository for radioactive waste in rock salt etc., requires a model of the solubility equilibria representing the experimental findings and interpolating data gaps in the hexary, oceanic system Na-K-Mg-Ca-Cl-SO_4-H_2O. All salt components, except for the calcium sulfate-containing salt minerals, possess high solubility, which means thermodynamic activity at high and very high ionic strength has to be described.

Table 3
Scheme for the categorisation of references in THEREDA.

Symbol	Description
1	Critical data collection with external review (e. g. CODATA, NEA-TDB, PSI-TDB-Report)
2	Internationally acknowledged review article (e. g. in IUPAC Solubility Data Series, Am. J. Sci. or Coord. Chem. Rev.)
3	Article in a peer-reviewed journal
4	Institutional report, Book, Ph.D. thesis, THEREDA-Journal (or similar publications, all without international or external review)

The background and the current state of the THEREDA database for the hexary oceanic salt system are outlined in the following sub-section 3.1.1. Subsequently, two sub-sections (3.1.2 and 3.1.3) follow, demonstrating how the oceanic data set can be applied to salt rock chemistry issues. In detail, sub-section 3.1.2 provides an example of the predictability of the development of solution compositions when in contact with saline formations, including stability of magnesia concrete as a sealing element, which has been empirically shown to be stable under saline conditions for over a century (Wasserdichte Verdämmung im Salzgebirge, 1902). And as an example of an extraction process, section 3.1.2 shows how the process conditions for the recovery of Trona, Na_2CO_3•$NaHCO_3$•$2H_2O$ (solution mining) can be derived and described.

3.1.1. The polythermal dataset for the oceanic salt system Na-K-Mg-Ca-Cl-SO_4-H_2O

In their seminal papers Harvie, Møller and Weare (Eugster et al., 1980; Harvie et al., 1984) demonstrated for T = 298 K that Pitzer's equations are suited to describe the solubility equilibria of the complete hexary oceanic system when appropriate adjustments of solubility constants and mixing parameters are introduced. The Pitzer equation formalism does not provide a functional form of the temperature dependence of the parameters. However, it initiated a large series of thermodynamic measurements at enhanced temperatures for binary and ternary electrolyte systems in the 1980s and 1990s years (e.g. Phutela et al. (1987); Pabalan and Pitzer (1988a, 1988b); Pitzer and Das (1998)), and particularly the series of isopiestic measurements at Oak Ridge National Laboratory (main authors: Holmes, Mesmer) and heat capacity and heat of dilution measurements, often initiated by Pitzer himself (e.g. Holmes et al. (1978, 1979; 1981); Holmes and Mesmer (1983); Busey et al. (1984); Holmes and Mesmer (1994)). With the focus to Geothermal energy and temperatures up to 250 °C the thermodynamic group of John Weare, Nancy Møller and Jerry Greenberg at the University of California, San Diego, developed Pitzer models for systems containing simple salts of chlorides and sulfates of sodium, potassium, calcium and its mixtures (Greenberg and Møller, 1989). Later on, Christov and Møller (2004a, 2004b) extended these models with bases components and acids. Magnesium was not considered in these models.

The extension to temperatures below 298 K was attempted first by Spencer et al. (1990), and later Marion and Kargel (2008) developed a series of Pitzer-based models for cold aqueous planetary geochemistry.

In the early 1990s the German Bundesamt für Strahlenforschung (BfS) - today's BGE - initiated a program to develop a Pitzer data file for the geochemistry of oceanic salt systems for temperatures up to about 373 K with the focus on description of the multicomponent solubility equilibria. This work was continued with THEREDA up to now.

For the development of the polythermal data set, using the "HMW model" (Harvie et al., 1984) as a 25 °C anchor, the temperature functions of binary parameters of Pitzer, Pabalan, Holmes, Mesmer, Greenberg and Møller (e.g. Pabalan and Pitzer (1987); Greenberg and Møller (1989); Holmes and Mesmer (1986, 1996)) were re-fitted to a NEA-conform T-function with an upper limit of 373 K. For $MgCl_2$ an entire new data evaluation has been performed. Subsequently, solubility isotherms in ternary, quaternary and the quinary oceanic system were evaluated step by step and mixing parameters as well as solubility constants were fitted. This was a lengthy trial and error process, where the solubility of every oceanic mineral in all systems was evaluated and respective parameter adjustments were applied, if necessary. The full

documentation of the procedures and results for the quinary system was deposited in the year 1998 at BfS. In the following years equilibria with calcium-containing minerals were included as well the bases NaOH, KOH, $Mg(OH)_2$, $Ca(OH)_2$ and acids HCl and H_2SO_4 (Altmaier et al., 2011; Voigt, 2020). Recently, the implementation of carbonate was started (Voigt, 2023).

Altogether, the development process involved reviewing all available solubility data in literature, their critical evaluation, and storage in ASCII format (up to now approx. 16′000 data points). Semi-automatic fitting procedures were applied to find an optimised set of Pitzer-coefficients and solubility constants. With the inclusion of acids (HCl, H_2SO_4) and bases (NaOH, KOH, $Mg(OH)_2$, $Ca(OH)_2$) in addition to CO_2/carbonate, the THEREDA model is the first database worldwide to allow the polythermal description of multi-component equilibria of all major components of the oceanic system including acidic and alkaline conditions in a temperature range of at least 0–100 °C.

During the development process some improvements for the oceanic system were made to the underlying 25°C-HMW model. Thus, the chemical formula of kainite was corrected ($4KCl{\cdot}4MgSO_4{\cdot}11H_2O$ instead of $KCl{\cdot}MgSO_4{\cdot}3H_2O$); the missing mineral goergeyite ($K_2SO_4{\cdot}5CaSO_4{\cdot}H_2O$) was included, which has a crystallisation field at 298 K; the solubility of KCl is described more correctly; the water activity of gypsum/anhydrite transition at NaCl saturation is shifted to the more acceptable value of 0.84–0.85 (instead of 0.775 in the HMW model); two additional aqueous solution species ($KMgSO_4^+$, $KCaSO_4^+$) have been implemented - this was necessary, in order to describe solubilities at enhanced temperatures.

To date, and in the future, the dataset is being developed and updated in line with the state of knowledge. New experimental data are critically evaluated and continuously tested for compatibility with the THEREDA model. Improvements are considered in new releases, if necessary.

This dataset for the extended polythermal oceanic salt system (Na-K-Mg-Ca-H-Cl-SO_4-OH-CO_2-HCO_3-CO_3-H_2O) represents the basis of THEREDA. All other chemical elements and phase constituents (actinides, rare earth metals, heavy metals, organic ligands and others) contained in THEREDA are incorporated into the oceanic model ensuring consistency regarding Pitzer parameters and aqueous speciation.

Exemplarily for the oceanic system, the solubility isotherms for sylvite (KCl) and carnallite ($KCl{\bullet}MgCl_2{\bullet}6H_2O$) are shown at various temperatures in the ternary system K^+, Mg^{2+} || Cl^- - H_2O (Fig. 1) and in the quaternary system Na^+, K^+, Mg^{2+} || Cl^- - H_2O in quasi-ternary representation (Fig. 2). In Fig. 3 co-saturation lines and crystallisation fields of typical minerals in Zechstein deposits (chapter 3.1.1) are presented at three temperatures for the quaternary reciprocal system Na^+, Mg^{2+} || Cl^-, SO_4^{2-} - H_2O. The model leads to a good to fairly good agreement with the experimental data.

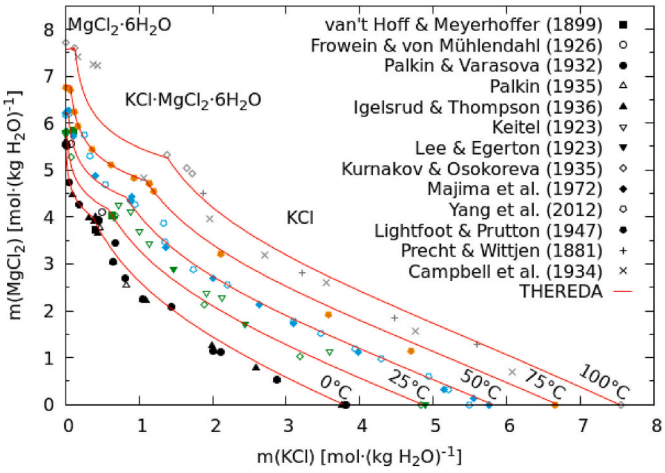

Fig. 1. Ternary system K^+, Mg^{2+} || Cl^- - H_2O with isotherms at 0 °C, 25 °C, 50 °C, 75 °C, and 100 °C. Calculations were performed using PHREEQC Interactive version 3.8.6.17100 (Campbell et al., 1934; Frowein and Von Mühlendahl, 1926; Igelsrud and Thompson, 1936; Keitel, 1923; Kurnakov and Osokoreva, 1935; Lee and Egerton, 1923; Lightfoot and Prutton, 1947; Majima et al., 1972; Palkin, 1935; Palkin and Varasova, 1932; Parkhurst and Appelo, 2013; Precht and Wittjen, 1881; van't Hoff and Meyerhoffer, 1899; Yang et al., 2012).

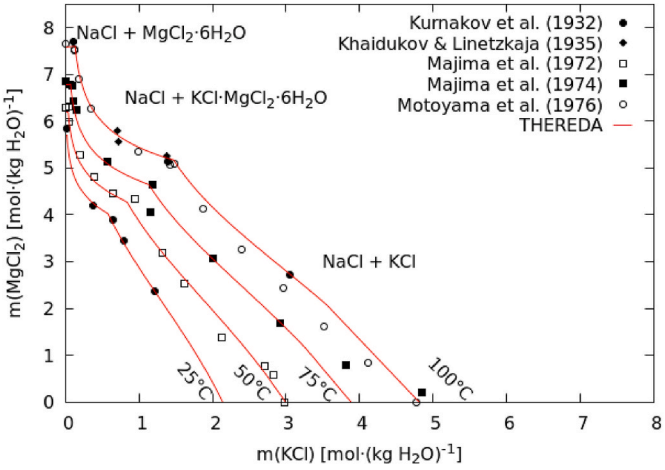

Fig. 2. Quaternary system Na^+, K^+, Mg^{2+} || Cl^- - H_2O at NaCl saturation with isotherms at 25 °C, 50 °C, 75 °C, and 100 °C in quasi-ternary representation for comparison with Fig. 1. Calculations were performed using PHREEQC Interactive version 3.8.6.17100 (Khaidukov and Linetzkaya, 1935; Kurnakov et al., 1932; Majima et al., 1972, 1974; Motoyama et al., 1976; Parkhurst and Appelo, 2013).

3.1.2. Development of the solution composition when groundwater penetrates via the shaft into a generic repository in the rock salt

In current repository concepts, such as for the host rock salt (steep or flat storage) (Bertrams et al., 2020a, 2020b), the repository is ultimately sealed for the long term by backfilling the shafts. The shaft sealing system is based on different sealing elements, the arrangement of which is orientated along the stratigraphy of the rock salt. This means that a building element will be installed whose material will not (or almost never) corrode in the event of a potential access of salt solution and can therefore fulfil a long-term sealing function at this location.

Nevertheless, after the installation of the shaft sealing system, a solution penetration is possible e.g. due to the failure of the shaft lining around the groundwater-bearing layers of the overburden. For the event of solution migration along the shaft surrounding zone through the horizons of the host rock salt to the deepest part of the shaft, THEREDA is used to calculate the resulting solubility equilibria with the salt minerals present in the contact zone. As the solution only migrates downwards very slowly due to the porosity and permeability in the contact zone, the deepest point of the shaft is expected to be reached after years to decades (based on the plausible assumptions that the shaft diameter is 6 m and the shaft depth is 840 m, the salt-bearing horizons are reached after 375 m (thickness of the overburden), the contour zone running radially around the sealed shaft is 0.5 m, has a porosity of 1 % and the assumed integral solution permeability of the contour zone is in the order of $k = 10^{-15}$ m^2). Due to the slow penetration rate of the solution, the adjustment of the solubility equilibrium is calculated horizontally, starting with the first salt-bearing layers and progressing step by step to the depth of the shaft. From the above parameters, a total pore volume of 47.48 m^3 can be calculated for the contact zone around the shaft in the salt-bearing horizons. The pore space in the contact zone represents the volume that could be filled with water. Thus, it is used as a plausible water volume for the following calculations. In other words,

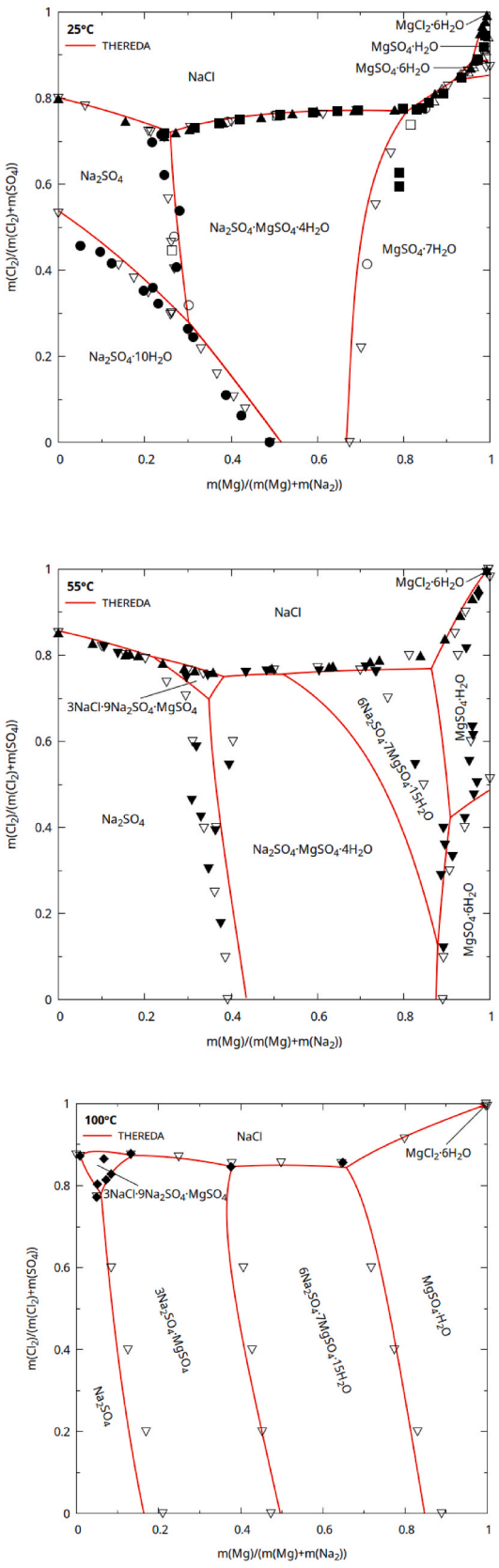

Fig. 3. Quaternary, reciprocal system Na^+, Mg^{2+} || Cl^-, SO_4^{2-} - H_2O. top: 25 °C, middle: 55 °C, and bottom: 100 °C. Experimental data from the literature: □ (Kurnakov and Žemčužny, 1924) ■ (Kurnakov and Opuchtina, 1930) ○ (Nikolaev and Burovaya, 1938) ● (Visjagin, 1939) △ (Solov'eva, 1946) ▲ (Autenrieth and Braune, 1960) ▽ (Pel'sh, 1953) ▼ (Yanat'eva, 1948) ⋄ (Orlova and Yanat'eva, 1963).

this volume of water is 'sent through once' without considering any additional flow from the overburden – as this is intended merely as a case study to demonstrate the calculability of salt geochemistry with THEREDA. For specific applications, the calculation process must be adapted to the relevant scenario.

The information on the composition of the salt rock surrounding the shaft with increasing depth, as it is generally found in the host rock horizons, is also required for the calculations (Fig. 4).

In the first calculation step, the 47.48 m^3 of water interact with the salt of the first horizon (z7 to z3TM combined). The resulting solution composition and quantity interacts with the next salt-bearing horizon z3AM, and further with z3RO, z3NA + z3HA, z2SF, and z2NA. The respective salt volume with its mineral phase fractions (Table 4) results from the layer thicknesses (Fig. 4) and the considered contour zone of 0.5 m radially surrounding the shaft. All calculations were performed assuming a temperature of 27 °C.

The obtained calculation results are shown in Fig. 5 with the corresponding numerical values given in Table 4 According to the results, as the water penetrates the first salt-bearing horizon (z7 to z3TM combined), consisting of halite and anhydrite, it dissolves the two phases until the saturation concentrations are reached, creating an appropriate cavity. Subsequently, the entire solution interacts with the next layer (Anhydritmittelsalz) z3AM, which already contains some potassium salt. The subsequent reactions involving sylvite (KCl), kieserite ($MgSO_4·H_2O$), carnallite ($KCl·MgCl_2·6H_2O$), and anhydrite ($CaSO_4$) lead to enrichment of the solution with Mg^{2+}, K^+, Cl^-, and SO_4^{2-} accompanied by crystallisation of further carnallite, polyhalite ($K_2SO_4·MgSO_4·2CaSO_4·2H_2O$), and some halite (NaCl). The hydrate formation (carnallite and polyhalite) dominates over the dissolution of the initial hydrate kieserite, so water is consumed from the solution. This leads to a decrease in the solution volume and an increase in the salt volume (the extent to which the pore volume in the contour zone changes up to this point and could therefore influence the process was not assessed here here). In contact with the subsequent layers z3RO (potash seam Ronneberg), z3NA - z3HA (Leine rock salt - Hauptanhydrit), z2SF (potash seam Staβfurt), and z2NA (Staβfurt rock salt) (Fig. 4), the solution does not undergo any further changes. Due to the relatively small amount of water or solution compared to the salt in the contour space, saturation very quickly occurs in relation to the potash salts present, i.e. these are no longer dissolved, so that the solution compositions no longer change and consequently no cavity formation or salt phase formation takes place.

Depending on the locally found stratigraphy and salt mineral content, deviating developments for the compositions of solution and salt minerals in equilibrium can result. The calculation results usually also require further interpretation as to whether the attainment of solubility equilibria (as calculated) can be classified as realistic if kinetic effects are kept in mind. For example, dissolution and crystallisation do not always take place at the same location. Supersaturated solutions can form, from which salts crystallise, reaching other locations. Equilibrium phases do not always crystallise, but sometimes metastable salts do. An example is the formation of metastable $MgSO_4$-hydrates instead of kieserite ($MgSO_4•H_2O$) (Xie et al., 2011). Salt chemistry experts can provide information on this.

THEREDA also allows to model interactions of salt solutions (brines) with Sorel concrete (magnesia construction material) as a potential shaft sealing element. Solubility equilibria can be reliably calculated for the binder phases of the Sorel building material ($xMg(OH)_2•yMgCl_2•zH_2O$ phases), as is shown by the good agreement of calculations using THEREDA with the experimental solubility data in the ternary system Mg^{2+} || Cl^-, OH^- - H_2O (Fig. 6) as well as in the quaternary system Na^+, Mg^{2+} || Cl^-, OH^- - H_2O at NaCl saturation (Fig. 7).

As an example, a 50 m long plug (⌀ 6 m, corresponding to the shaft diameter) is considered, placed in the z2NA-layer (deepest shaft) following the previous calculation for this stratigraphy in the contour zone. The calculation of the equilibration between the salt, the solution

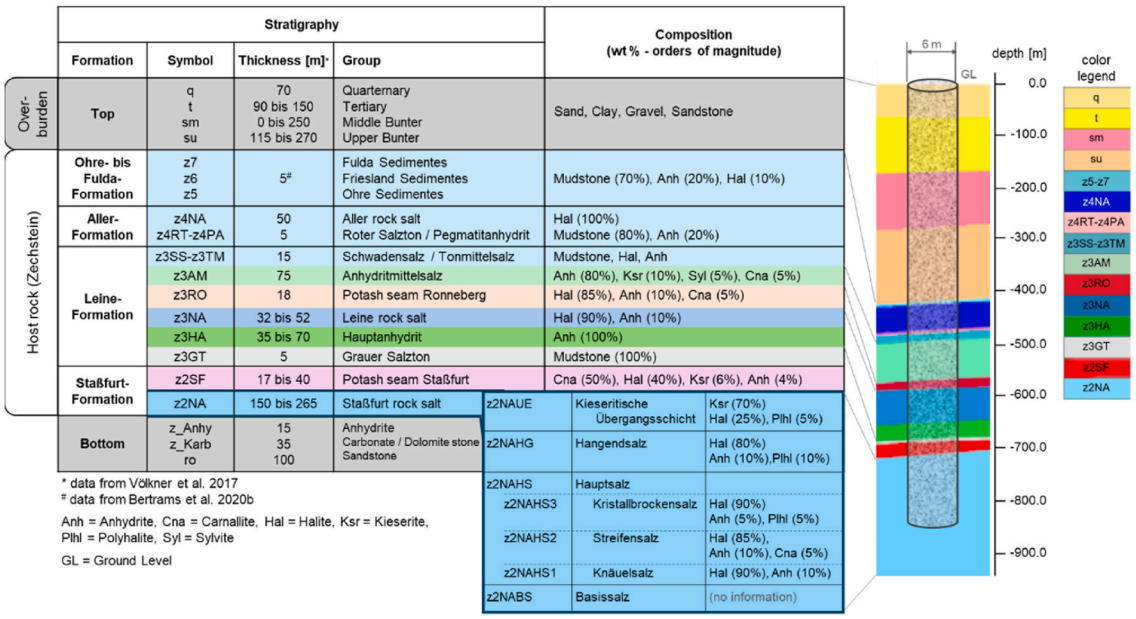

Fig. 4. Host rock salt in stratiform storage (Bertrams et al., 2020b) which can be encountered in the shaft depending on depth. Composition: qualitatively according to (Keller, 2007); quantitatively based on Bornemann and Fischbeck (1987), Bornemann et al. (2008), Schramm (2013).

in the contour zone, and the building material (assumed to be the 3-1-8 binder phase, 3 $Mg(OH)_2 \bullet MgCl_2 \bullet 8H_2O$) with a plug length of 50 m (all initial information is provided in Table 5) shows that no conversions take place, as the composition of neither the solution nor the solid phases (host rock minerals and binder phase of Sorel concrete) changes (Fig. 8 and Table 5). As Table 5 shows, a low OH^- concentration forms in the solution due to the equilibration with the 3-1-8 Sorel phase. The stability of the Sorel concrete is indicated by the solid-solution-equilibrium.

3.1.3. *Application in solution mining*

In addition to nuclear disposal in rock salt, THEREDA can also be used to address issues relating to solution mining (*in situ* leaching or *in situ* recovery), a technique for recovering minerals (as raw materials, chemicals) through boreholes drilled into a deposit. The target material is dissolved, and the resulting brine is pumped to the surface for further processing. For many centuries, this method has been successfully used in the mining of salts. Particularly halite (NaCl) with its relatively simple phase chemistry has been extracted this way. Today, however, there is growing interest in salts with more complex dissolution behaviour (potash, trona, sodium sulphates, magnesium chloride, etc.) (Warren, 2016). So-called "blinding" (formation of a layer of less soluble salt covering the cavern surface) often causes difficulties, which means that the target mineral becomes shielded. Dealing with such challenges requires a thorough understanding of brine phase chemistry. Phase equilibria and their temperature sensitivity form a basis for the successful operation of a solution mine.

The THEREDA model provides a powerful tool for predicting, optimising, and monitoring solution mining processes for a wide range of evaporitic salts. Polythermal phase equilibrium calculations are supported in the temperature range from 0 to 100 °C.

In the following, the example of trona ($Na_2CO_3 \bullet NaHCO_3 \bullet 2H_2O$) is chosen to demonstrate the capabilities of THEREDA in the context of solution mining. Trona is an important raw material in the production of sodium carbonate-containing substances (soda ash Na_2CO_3, nahcolite $NaHCO_3$, also referred to as "baking soda") and solution mining is frequently used for its recovery (Warren, 2016). In the history of trona exploitation due to insufficient knowledge of the chemical behaviour of the system, the formation of less soluble nahcolite led to the blinding of surfaces (Haynes and Henry, 1997). As a result, dissolution of the targeted trona slowed down or was even prevented. This observation may be explained by phase equilibria in the sodium carbonate system Na_2CO_3-$NaHCO_3$-H_2O and be avoided by a suitable process management.

Experimental solubility data have been published in the system for selected temperatures. However, a complete phase diagram is preferable for further considerations like identification of conditions favourable for specific dissolution/precipitation behaviours. The THEREDA dataset can be applied to calculate such a diagram (Fig. 9). Also, process simulation is possible. The following scenarios are of interest if nahcolite blinding is to be avoided:

(1) The dissolution of trona in pure water
(2) The dissolution of trona in aqueous Na_2CO_3 solution
(3) The dissolution of trona in aqueous NaOH solution

(1) When trona is dissolved in pure water, the development of solution concentration follows path A-A′ in the phase diagram (blue path in Fig. 9). As soon as the 40 °C isotherm is reached (point B), unwanted nahcolite precipitates until saturation with trona is reached at point C. Thermodynamic modelling with THEREDA yields specific amounts of substances as listed in Table 6: At 40 °C 492 g of trona is dissolved in 1 kg of pure water; at the same time, 100 g nahcolite is precipitated and shields the trona surface from further dissolution. Operating at higher temperatures helps to reduce the mass of unwanted nahcolite: At 60 °C only 67 g of nahcolite precipitates while 490 g of trona is dissolved in 1 kg of pure water (path A-B′-C′ in Fig. 9).
(2) Dissolving trona in aqueous Na_2CO_3 solutions instead of pure water helps to further reduce nahcolite precipitation. If 15 wt% Na_2CO_3 solution at 40 °C is used as a solvent (red path D-E in Fig. 9), 134 g trona (167 g at 60 °C) can be dissolved in 1 kg of solution and no co-precipitation of unwanted substances occurs (Table 6).
(3) Another option to avoid nahcolite precipitation is the use of NaOH solution as a solvent (green path F-G in Fig. 9). In a 4 wt% NaOH solution at 40 °C, 358 g trona will be dissolved (395 g at 60 °C), while no unwanted phases are blinding the surface.

Such a comparison of different processes can be conveniently done with calculations using THEREDA. Solution concentrations, mass and

Table 4
Initial and resulting numerical values of the THEREDA calculation for the development of solution composition and salts in equilibrium at 27 °C according to Fig. 5. The volumes of the salt components of the contour zone (host rock) are given before and after solution contact, the difference (in %) is shown in Fig. 5.

Host rock contour zone					Ground water ingress	Solid-solution equilibrium setting									
						Salts		Solution composition							
Thickness / m		Salt phases	V* / m³	wt / %	m³		V / m³	w (H_2O) / kg	molality [mol / kg H_2O]					
									Na^+	K^+	Mg^{2+}	Ca^{2+}	Cl^-	SO_4^{2-}
z3TM-z7	75	Hal	682.30	86.84	47.48 **	Hal	674.44	47'477.3	6.143	-	-	0.038	6.143	0.038
		Anh	75.81	13.16		Anh	75.73							
			758.11				750.17							
z3AM	75	Anh	606.48	84.41		Anh	573.28	16'815.6	0.267	0.153	4.891	8.9e-4	9.626	0.288
		Ksr	75.81	9.20		Ksr	36.73							
		Syl	37.91	3.54		Hal	7.73							
		Cna	37.91	2.86		Cna	87.24							
			758.11			Plhl	78.97							
							783.96							
z3RO	18	Hal	154.65	83.06		Hal	154.65	16'815.6	0.267	0.153	4.891	8.9e-4	9.626	0.288
		Anh	18.19	13.33		Anh	18.15							
		Cna	9.10	3.61		Cna	9.10							
			181.95				181.95							
z3NA-z3HA	122	Hal	616.59	42.30		Hal	616.59	16'815.6	0.267	0.153	4.891	8.9e-4	9.626	0.288
		Anh	616.59	57.70		Anh	616.59							
			1'233.19			Cna	3.79e-9							
							1'233.19							
z2SF	40	Hal	230.46	59.47		Hal	230.46	16'815.6	0.267	0.153	4.891	8.9e-4	9.626	0.288
		Cna	101.08	19.26		Cna	101.08							
		Ksr	64.69	19.85		Ksr	64.69							
		Anh	4.04	1.42		Anh	4.04							
			400.28			Plhl	2.1e-10							
							400.28							
Z2NA	130	Hal	1'051.24	76.14		Hal	1'051.24	16'815.6	0.267	0.153	4.891	8.9e-4	9.626	0.288
		Ksr	131.40	11.32		Ksr	131.40							
		Plhl	65.70	6.06		Plhl	65.70							
		Anh	65.70	6.49		Anh	65.70							
			1'314.05			Cna	2.6e-13							
							1'314.05							

* Volume of the minerals corresponding to layer thickness and 0.5 m depth contour zone surrounding the shaft.

salt phases: Anh = Anhydrite, Cna = Carnallite, Hal = Halite, Ksr = Kieserite, Plhl = Polyhalite, Syl = Sylvite

Molar masses and densities for the salts as included in THEREDA (Anh = 2.96, Cna = 1.602, Hal = 2.17, Ksr = 2.58, Plhl = 2.763, Syl = 1.988 g/cm³).

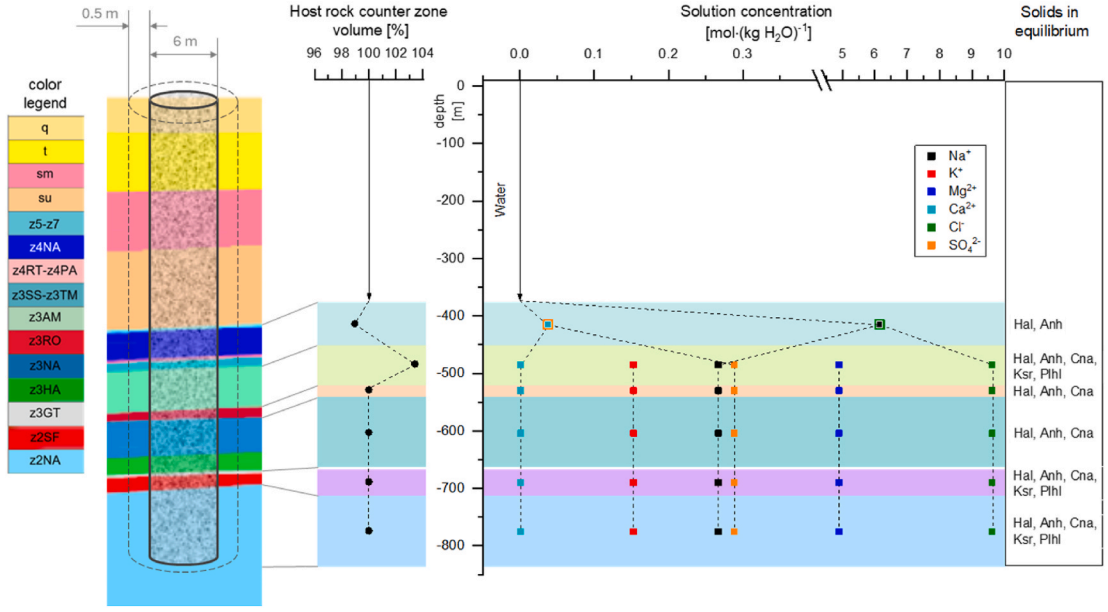

Fig. 5. THEREDA modelling results for the development of solution composition and salts in equilibrium at 27 °C (all associated numerical values are given in Table 4), as well as volume development of the contour zone (0.5 m) surrounding the shaft ("Host rock counter zone volume" is calculated from the salt volume before and after equilibrium setting (Table 4); stratigraphy with general mineral content see Fig. 4. Abbreviations: Hal = Halite, Anh = Anhydrite, Cna = Carnallite, Plhl = Polyhalite, Ksr = Kieserite. Calculations were performed using PHREEQC Interactive version 3.8.6.17100 (Parkhurst and Appelo, 2013).

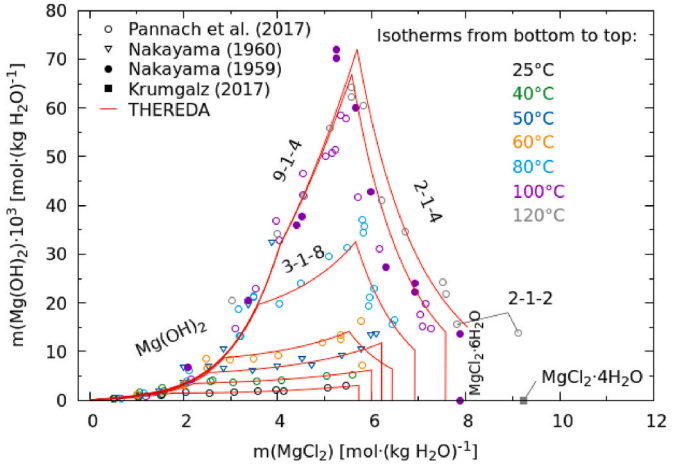

Fig. 6. Solubilities in the ternary system Mg^{2+} || Cl^-, OH^- - H_2O from 25 to 120 °C. 3-1-8 = 3 $Mg(OH)_2$•$MgCl_2$•$8H_2O$; 9-1-4 = 9 $Mg(OH)_2$•$MgCl_2$•$4H_2O$; 2-1-4 = 2 $Mg(OH)_2$•$MgCl_2$•$4H_2O$; 2-1-2 = 2 $Mg(OH)_2$•$MgCl_2$•$2H_2O$. Calculations were performed using PHREEQC Interactive version 3.8.6.17100 (Krumgalz, 2017; Nakayama, 1959, 1960; Pannach et al., 2017; Parkhurst and Appelo, 2013).

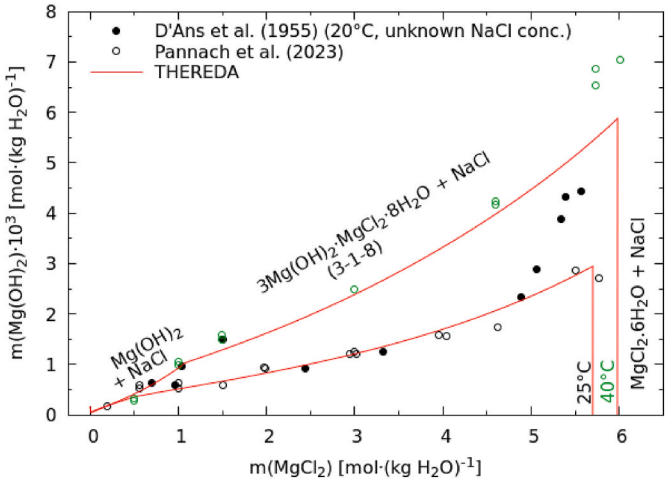

Fig. 7. Solubilities in the quaternary system Na^+, Mg^{2+} || Cl^-, OH^- - H_2O at NaCl-saturation and 25 and 40 °C. Calculations were performed using PHREEQC Interactive version 3.8.6.17100 (D'Ans et al., 1955; Pannach et al., 2023; Parkhurst and Appelo, 2013).

composition of solid phases formed, water activities, pH values, and further data can easily be obtained for every single process step.

Especially if further salt components (impurities) in the system must be considered, a simple application of phase diagrams is impossible, and thermodynamic modelling has to be applied, provided such impurities are included in the database. THEREDA facilitates phase diagram calculations and process simulations for a wide range of salts in the extended oceanic system.

3.2. Radionuclide chemistry

3.2.1. Uranium

Uranium is the main element in spent fuel and the largest mass inventory in nuclear waste. Other sources are the environmental contamination from nuclear accidents and depleted uranium ammunition, uranium mining and processing, and as NORM (natural occurring radioactive material), especially from rare earth elements (REE) mining and fertiliser production. Relevant oxidation states under oxidising and reducing conditions are the more mobile U(VI) (as UO_2^{2+}) and the less mobile U(IV) (as U^{4+}), respectively.

One objective of THEREDA is to enable the modelling of the dissolution of primary nuclear fuel materials and the possible formation of solid U secondary phases in the U(IV)/U(VI) system at high ionic strengths in the oceanic salt system over a wide pH range. Furthermore, scoping calculations for chosen sub-systems (e.g., Pourbaix diagrams for radionuclides) should be possible.

A consistent Pitzer dataset for U(IV) and U(VI) was derived covering the hydrolysis species and (hydroxo)carbonates. Solubility constants for

Table 5
Numerical values for Fig. 8: THEREDA modelling of the equilibrium setting between access-solution, host rock salt, and Sorel concrete plug (binder phase 3-1-8) at 27 °C.

Host rock contour zone						Solid-solution equilibrium setting									
						Salts		Solution composition							
Thickness / m		Salt phases	V* / m^3	Fraction / wt. %			V / m^3	w (H_2O) /kg	molality [mol / kg H_2O]						
									Na^+	K^+	Mg^{2+}	Ca^{2+}	Cl^-	SO_4^{2-}	OH^-
z2NA	80	Hal	646.92	76.14		Hal	646.92	16'815.6	0.267	0.153	4.891	8.9e-4	9.626	0.288	-
		Ksr	80.86	11.32		Ksr	80.86								
		Plhl	40.43	6.06		Plhl	40.43								
		Anh	40.43	6.49		Anh	40.43								
			808.65				808.6								
	50	Hal	404.32	76.14	Sorel concrete as shaft sealing element	Hal	404.32	16'817.5	0.266	0.153	4.893	8.9e-4	9.626	0.289	4.7e-3
		Ksr	50.54	11.32		Ksr	50.54								
		Plhl	25.27	6.06		Plhl	25.27								
		Anh	25.27	6.49		Anh	25.27								
			505.40				505.40								
		3-1-8	18.54*			3-1-8	18.54								

** The volume of the 3-1-8 binder phase (18.54 m^3 = 34.48 t; density of 3-1-8 phase = 1.86 g/cm^3) is derived from a possible concrete composition of 20% binder phase and 80% inert aggregates (like crushed rock salt and/or sand/gravel) and correspond to the volume of the binder phase in the surface region of the concrete plug (10 cm depth into the plug (∅ 6 m, H: 50 m) via the lateral surface, which interacts with the solution from the previous calculation step for this stratigraphy in the contour zone.*

Table 6
Masses of solids processed in trona solution mining as calculated with THEREDA.

Temp./ °C	Solvent	Max. dissolved trona/g	Type of co-precipitating salt	Mass of co-precipitating salt/g	Path in phase diagram
40	Pure water	492	nahcolite	100	A-B-C
	15 wt% Na_2CO_3 solution	134	–	0	D-E
	4 wt% NaOH	358	–	0	–
60	Pure water	490	nahcolite	67	A-B′-C′
	15 wt% Na_2CO_3 solution	167	–	0	–
	4 wt% NaOH	395	–	0	F-G

the solubility-determining solid phases were selected for THEREDA. As examples, the capability of THEREDA to reproduce the solubility of metaschoepite UO_3•2H_2O, clarkeite $Na_2U_2O_7$•H_2O (Fig. 10), as well as U(OH)$_4$(am) and UO_2·H_2O(ncr) (Fig. 11) over a wide range of molal H^+-concentration is demonstrated. The corresponding Pitzer activity models were either taken from the literature (U(VI) (Yalcintas et al., 2019),) or newly derived in the context of the THEREDA project (U(IV) (Yan et al., 2024),). Note that the selection of the U(IV) phases U(OH)$_4$(am) (am = amorphous) and UO_2·H_2O (ncr) (ncr = nano-crystalline) basically reflects the impact of Ostwald ripening on the effective solubility of a given solid phase. This process is especially relevant for strongly hydrolysing metal ions such as An(III) and An(IV).

Other solid phases, if their occurrence in natural environments is evident, were added, such as carbonates, phosphates, or sulfates. Where possible, thermodynamic data were adopted from the NEA TDB (Ragoussi and Brassinnes, 2015) or other sources. Particular attention was paid to solid phases detected in experiments or observed in natural geological environments. However, systematic solubility studies for the latter are often missing and calculated solubilities must be regarded with caution.

3.2.2. Other actinides in THEREDA

Besides uranium, thermodynamic data for the main actinides (An) of relevance in the context of nuclear waste disposals are also selected for THEREDA. This includes Np, Pu, and Am, extending also to Th and Cm. The current selection covers the oxidation states + III (Am, Cm), +IV (Np, Pu, Th), and +V (Np). Note, the +VI oxidation state is only considered for uranium so far. Solubility and hydrolysis are systematically covered for all these systems, whereas thermodynamic data for the actinide-carbonate system are only selected for Am(III), Cm(III), Np(IV), and Pu(IV). A new release in preparation will update the thermodynamic selection for the An(IV)–OH–CO_3 system (with An = Th, U, Np, Pu) in alkaline to hyperalkaline conditions, considering the update volume of the NEA-TDB (Grenthe et al., 2020) as well as new thermodynamic data available for these systems (Altmaier et al., 2005, 2006; Schepperle, 2020; Kobayashi et al., 2021).

The formation of ternary aqueous complexes Ca–An–OH(aq) has been confirmed in intermediate to high $CaCl_2$ concentrations for the actinides in the oxidation states + III, +IV, and +V. Thermodynamic data available for these systems are implemented in THEREDA, including equilibrium constants and corresponding Pitzer-coefficients. Fig. 12 exemplarily shows the solubility of Np(OH)$_4$(am) in 5.26 m

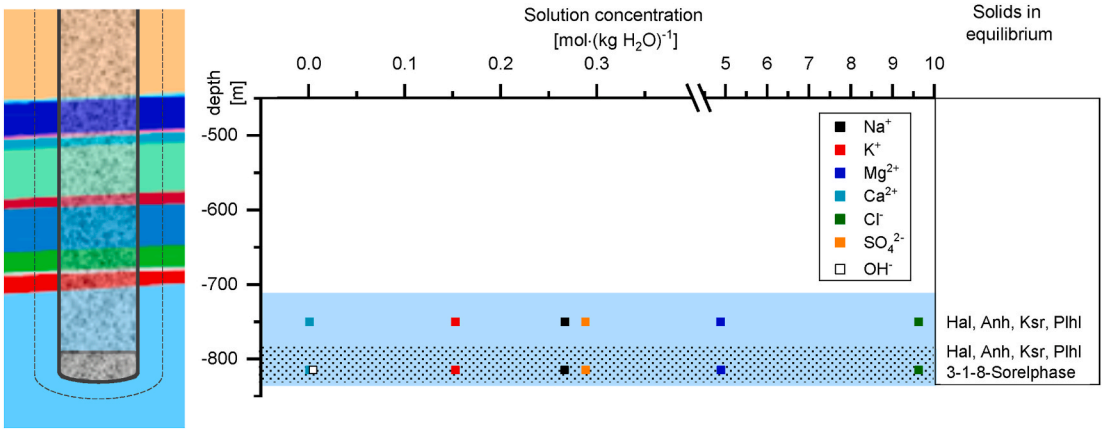

Fig. 8. THEREDA modelling of the equilibration of access-solution with salt rock and Sorel concrete (binder phase 3-1-8) at 27 °C in continuation of Fig. 5 with the addition of the Sorel concrete element (plug); corresponding numerical values in Table 5 Abbreviations: Hal = Halite, Anh = Anhydrite, Cna = Carnallite, Plhl = Polyhalite, Ksr = Kieserite. Calculations were performed using PHREEQC Interactive version 3.8.6.17100 (Parkhurst and Appelo, 2013).

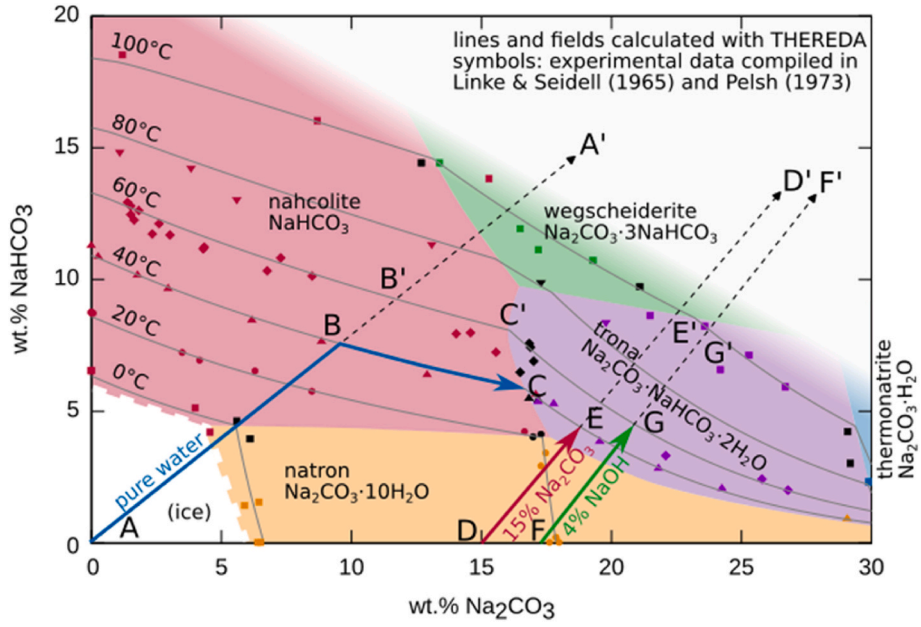

Fig. 9. Ternary polythermal phase diagram for the system Na_2CO_3-$NaHCO_3$-H_2O. Symbols: experimental solubility data from the literature (Linke and Seidell, 1958; Pel'sh, 1973), colours of the symbols are chosen according to the solid phase in equilibrium with the solution. Black indicates two salt points. Isotherms, stability fields and reaction paths were calculated using the THEREDA model and the code PHREEQC (Interactive version 3.8.6.17100 Parkhurst and Appelo, 2013). Blue arrow: Dissolution of trona in pure water at 40 °C, red arrow: Dissolution of trona in a 15 wt% Na_2CO_3 solution at 40 °C, green arrow: Dissolution of trona in a 4 wt% NaOH solution at 60 °C. Points A′, D′ and F′ are indicating the direction towards the composition of trona (46.89 wt% Na_2CO_3, 31.17 wt%. $NaHCO_3$).

$CaCl_2$ experimentally determined in Altmaier et al. (2008), together with the solubility calculated by THEREDA.

The + V oxidation state of the actinides is usually considered as the most soluble and mobile. However, in the presence of Ca, ternary solid phases Ca–Np(V)–OH(s) have been shown to impose significantly low Np(V) concentrations in hyperalkaline pH systems containing Ca (Fellhauer et al., 2016a, 2016b), even in the range of moderate Ca concentrations expected in cementitious systems, e.g., 20 mM. Fig. 13 shows the solubility of Np(V) in 0.25 and 5.26 m $CaCl_2$ solution calculated using THEREDA, compared with the experimental solubility data reported in Fellhauer et al. (2016b). In both $CaCl_2$ systems, the solubility of Np(V) is controlled by the solid phase $Ca_{0.5}NpO_2(OH)_2 \bullet 1.3H_2O$, which in 0.25 m $CaCl_2$ solutions with $pH_m \approx 11.2$ defines a solubility as low as [Np(V)] ~ $10^{-8.5}$ m.

Carbonate is a hard Lewis base forming strong complexes with the actinides. In alkaline to hyperalkaline systems containing carbonate, the formation of ternary complexes of the type An–OH–CO_3 is known and is selected in THEREDA for An(IV) (with An = Th, Np, Pu) and Np(V). For Pu(IV), the ternary complex $Pu(OH)_2(CO_3)_2^{2-}$ prevails in alkaline systems at low carbonate concentrations, whereas the binary complexes $Pu(CO_3)_4^{4-}$ and $Pu(CO_3)_5^{6-}$ dominate the aqueous speciation of Pu(IV) at high carbonate concentrations (Fig. 14).

3.2.3. *Technetium*

^{99}Tc is a fission product of ^{235}U and ^{239}Pu, which forms with high yields in nuclear reactors. It is a β-emitting, long-lived radionuclide ($t_{1/2} \approx 2.13 \bullet 10^5$ a). Tc can be found in a variety of oxidation states ranging from –I to + VII, although Tc(IV) and Tc(VII) are the ones primarily controlling the potential release of this radionuclide from a repository into the biosphere. Tc(VII) predominates in mildly reducing to oxidising conditions in the form of the anionic, highly mobile pertechnetate ion (TcO_4^-). In the very reducing conditions relevant in underground

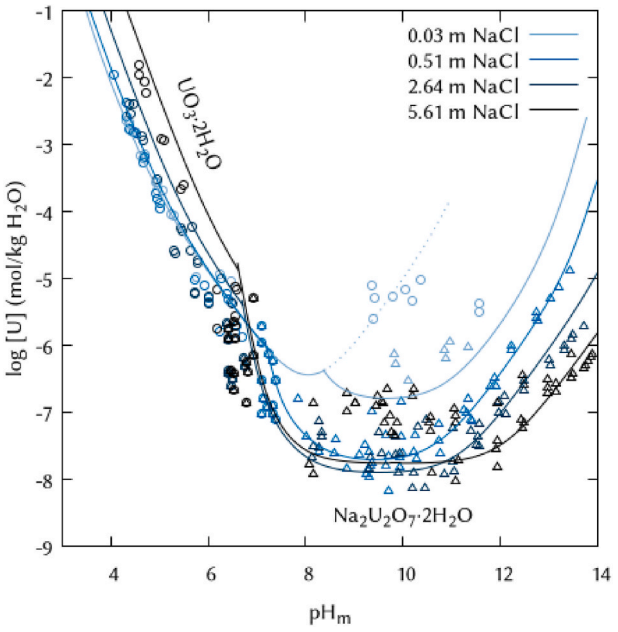

Fig. 10. Solubility of metaschoepite ($UO_3 \bullet 2H_2O$, circles) and clarkeite ($Na_2U_2O_7 \bullet 2H_2O$, triangles) in NaCl solutions. All experimental data taken from Altmaier et al. (2017). Lines: Calculation with THEREDA using Geochemist's Workbench (React) version 18.0.2 (Bethke, 2021).

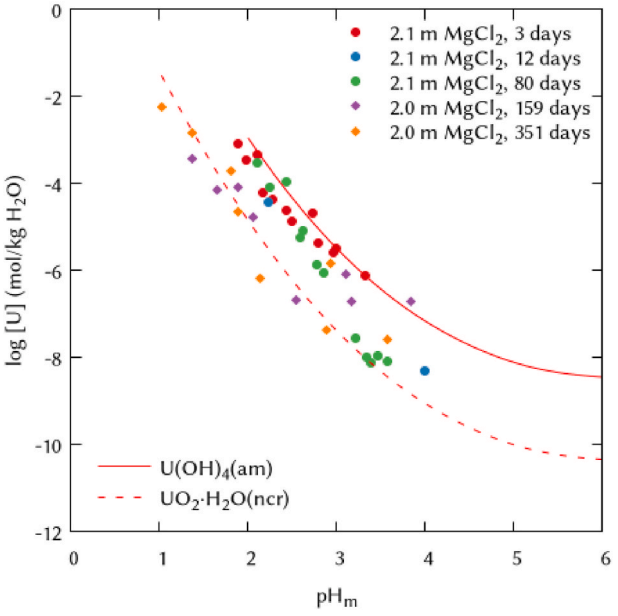

Fig. 11. Solubility of amorphous and nanocrystalline uranium(IV) hydroxide in 2/2.1 molal $MgCl_2$ solution. All experimental data taken from Rai et al. (1997) (circles) and Yan et al. (2024) (diamonds). Lines: Calculation with THEREDA using Geochemist's Workbench (React) version 18.0.2 (Bethke, 2021).

repositories for nuclear waste disposal, the oxidation state + IV is expected to control the aquatic chemistry of technetium. Tc(IV) is characterised by strong hydrolysis, the formation of sparingly soluble hydrous oxides, TcO_2(am, hyd), as well as a strong interaction with carbonate (Grenthe et al., 2020). The first release of THEREDA including Tc was issued in 2016, mostly based on the solubility study in dilute to concentrated NaCl, $MgCl_2$, and $CaCl_2$ solutions by Yalçıntaş et al. (2016). This model has been updated for the upcoming THEREDA release (see also Kiefer et al. (2025)), considering all reliable solubility

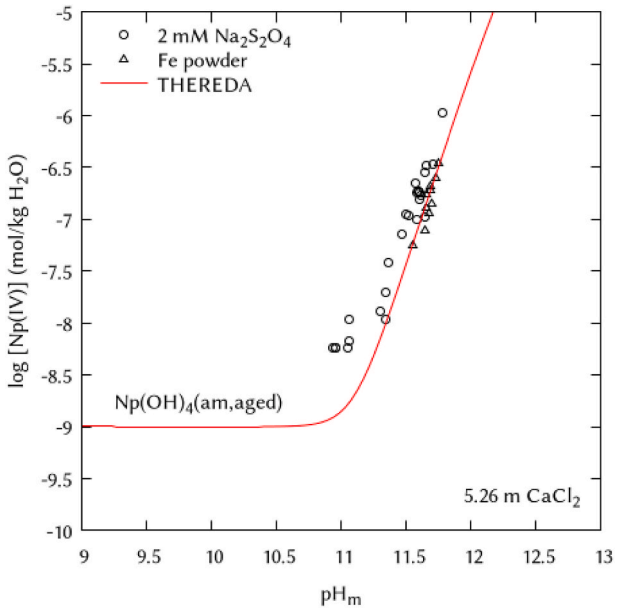

Fig. 12. Solubility of amorphous Np(IV) hydroxide in 5.26 m $CaCl_2$, using different reducing agents. Experimental data (circles and triangles) from Altmaier et al. (2008). Thermodynamic selection in Altmaier et al. (2008)and Fellhauer et al. (2009) was based on experimental data obtained in 1.02 m $CaCl_2$ ($Na_2S_2O_4$), 2.11 m $CaCl_2$ (with Fe powder), and 5.26 m $CaCl_2$ (two series, with Fe and $Na_2S_2O_4$). Line: Calculation with THEREDA using Geochemist's Workbench (React) version 18.0.2 (Bethke, 2021).

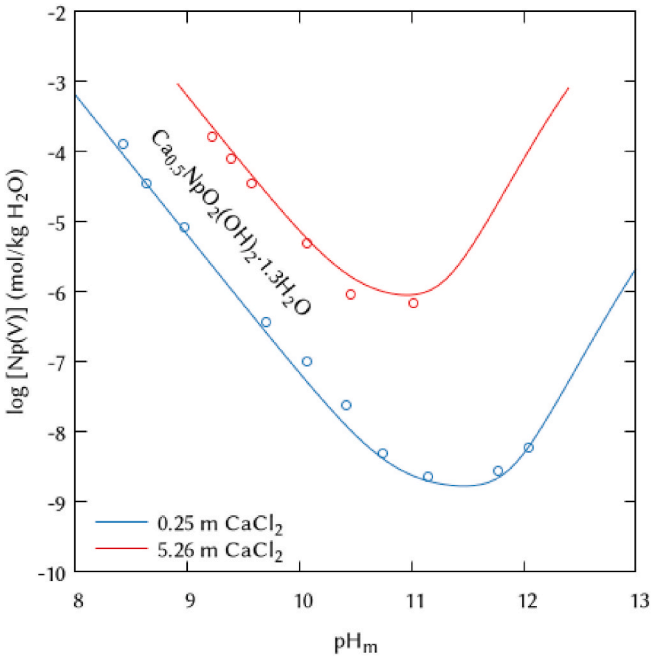

Fig. 13. Solubility of $Ca_{0.5}NpO_2(OH)_2 \bullet 1.3H_2O$ in 0.25 and 5.26 m $CaCl_2$ solution. Experimental data (circles) from Fellhauer et al. (2016b). Lines: Calculation with THEREDA using Geochemist's Workbench (React) version 18.0.2 (Bethke, 2021).

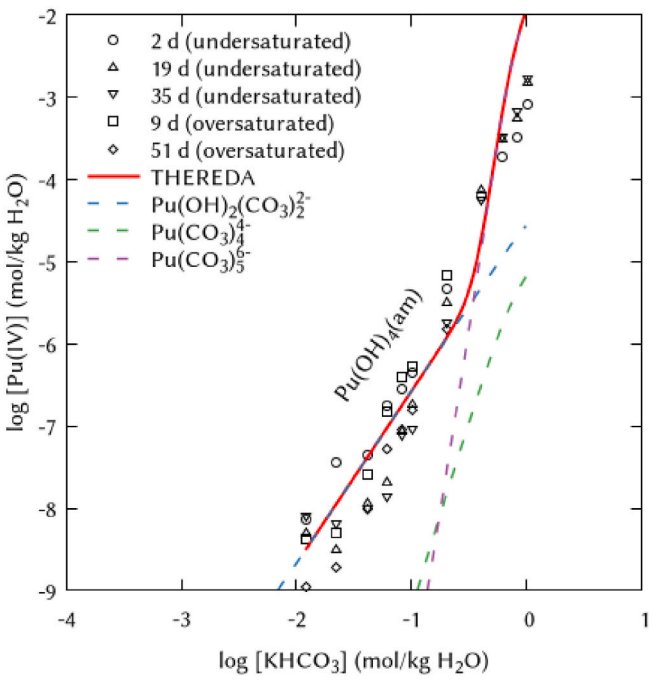

Fig. 14. Solubility of $Pu(OH)_4(am)$ in $KHCO_3$ solution. Experimental data reported in Rai et al. (1999). Solid and dashed lines: Calculation with THEREDA using Geochemist's Workbench (React) version 18.0.2 (Bethke, 2021).

data sources available to date in NaCl, KCl, $MgCl_2$, $CaCl_2$ as well as in dilute solutions (Eriksen et al., 1992; Liu et al., 2007; Yalçıntaş et al., 2016; Baumann et al., 2017) and accounting for the updated Tc thermodynamic data selection in the NEA-TDB (Grenthe et al., 2020). The resulting model explains all available solubility data in dilute to concentrated NaCl, KCl, $MgCl_2$, $CaCl_2$ solutions well (see Fig. 15 left, exemplarily showing Tc(IV) solubility in selected $MgCl_2$ solutions).

Additionally, Fig. 15 (right) also shows the performance of the model with respect to solubility experiments in "simulated reference systems", i.e., artificial cement pore water, cement simulates exposed to NaCl brine, Canadian reference groundwater or WIPP generic weep brine. The reader is referred to the original publication (Baumann et al., 2017) to account for the composition of the "simulated reference systems". Future THEREDA releases will extend the Tc(IV) Pitzer model to the carbonate system.

3.2.4. Selenium

^{79}Se with a half-life of 327′000 years is an important fission product of ^{235}U naturally occurring in various oxidation states (+VI, +IV, ±0, –II). Many Se(VI) and Se(IV) mineral phases are highly soluble making

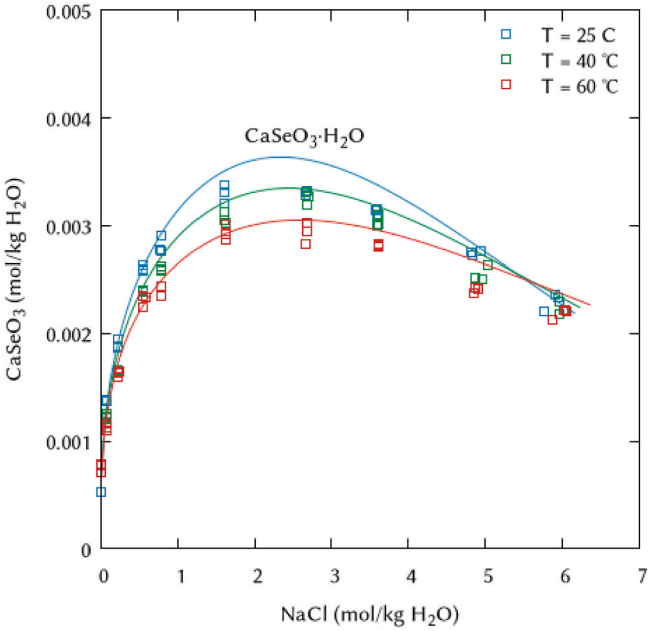

Fig. 16. Solubility of $CaSeO_3 \cdot H_2O$ in NaCl solution at 25 °C, 40 °C, and 60 °C. Experimental data (squares) reported in Bischofer et al. (2016), Olin et al. (2005) and calculations with THEREDA (lines) using Geochemist's Workbench (React) version 18.0.2 (Bethke, 2021).

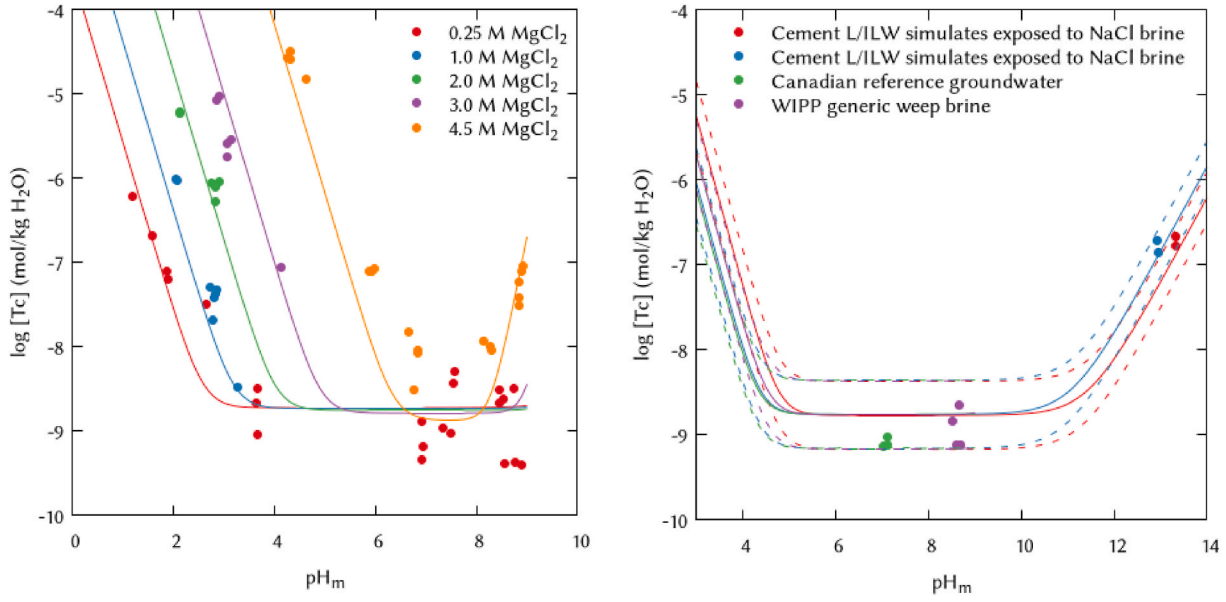

Fig. 15. Solubility of $TcO_2 \cdot 0.6H_2O$(am): left: in 0.25, 2.0, and 4.5 mol/L $MgCl_2$. Experimental data (circles) from Yalçıntaş et al. (2016) and calculations (lines) performed using the THEREDA release 2025; right: Comparison of experimental solubility data reported in Baumann et al. (2017) for "simulated reference systems" (artificial cement pore water, cement L/ILW simulates exposed to NaCl brine, Canadian reference groundwater and WIPP generic weep brine) and calculated (lines) using the upcoming THEREDA release. Calculations were performed using Geochemist's Workbench (React) version 18.0.2 (Bethke, 2021).

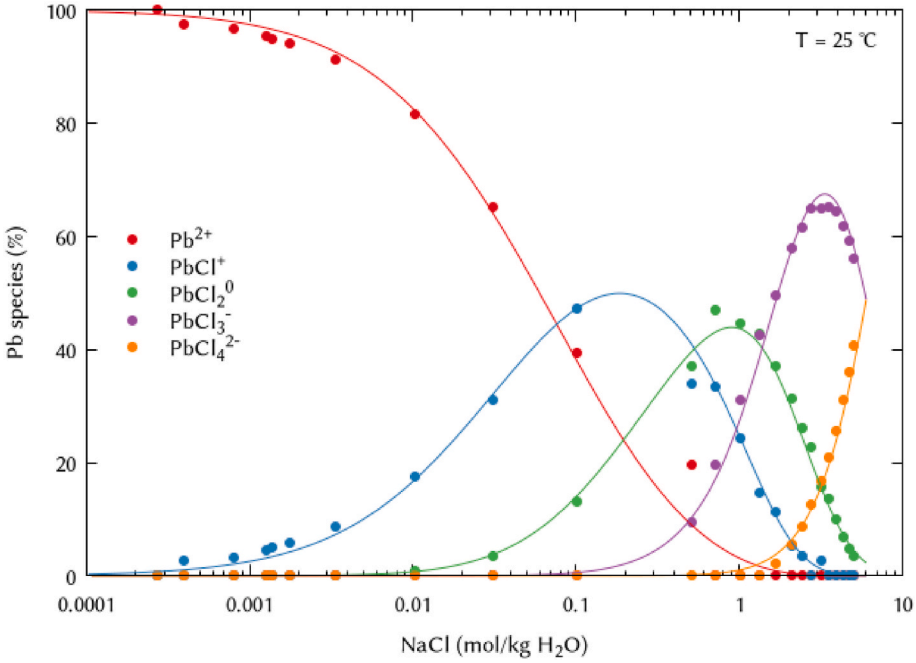

Fig. 17. Speciation of lead as a function of chloride concentration at 25 °C and with the addition of 0.0001 mol HCl. Species contributing less than 1 % are not depicted. Points: Experimental data measured by Hagemann (1999). Lines: Calculation with THEREDA using Geochemist's Workbench (React) version 18.0.2 (Bethke, 2021).

selenium very mobile under oxidising conditions. Solubility limiting phases under such conditions (e.g. $E_h > 250$ mV at pH ≈ 5, $E_h > 100$ mV at pH ≈ 7, $E_h > -50$ mV at pH ≈ 9) are $CaSeO_3{\cdot}H_2O$ and $MgSeO_3{\cdot}6H_2O$ (Bischofer et al., 2016; Bok, 2021). In addition to the safety of a repository for radioactive waste, selenium plays a major role in the environment and for humans. It can cause medical problems in cases of both over- and undersupply.

THEREDA contains a polythermal dataset to calculate the solubility of Se(+VI, +IV) phases in the oceanic salt system. The present model was tested in the temperature range from 0 to 100 °C. Additionally, the oxide phases SeO_2(cr) and SeO_3(cr) have been added to the dataset using thermodynamic data from the NEA-TDB (Olin et al., 2005). Fig. 16 demonstrates the calculation of $CaSeO_3{\cdot}H_2O$ in NaCl solutions at various temperatures.

At present, THEREDA does not contain data for either elemental Se (monoclinic, trigonal, amorphous) or for Se(−II) yet. This is due to a lack of proper solubility data in saline solutions.

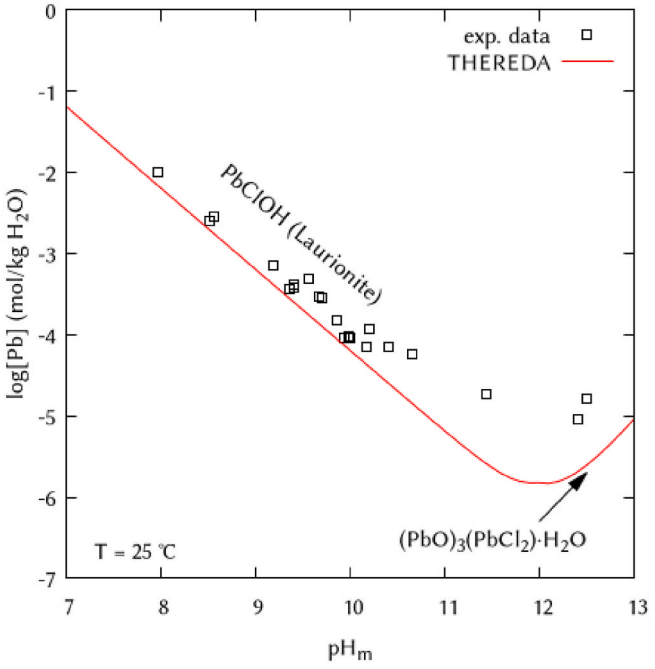

Fig. 18. Solubility of Pb(II) in solutions saturated with NaCl and $CaSO_4$ at 25 °C. Points: Experimental data measured by Hagemann (2024). Lines: Calculation with THEREDA using PHREEQC Interactive version 3.8.6.17100 (Parkhurst and Appelo, 2013).

3.3. *Non-radioactive inorganic contaminants*

3.3.1. *Lead*

Many radioactive waste types, waste containers, and other technical materials in a repository contain heavy metals and other chemotoxic elements that can lead to adverse effects on the quality of water resources. Among these, the chemical elements lead and zinc are currently included in THEREDA. The model to describe their properties in solutions containing Na, K, Mg, Cl, OH^-, and SO_4^{2-} at 25 °C is mainly based on Hagemann (2024).

Lead occurs in natural systems practically only in the oxidation state Pb(II). In chloride-rich solutions, Pb^{2+} forms chloro complexes of the type $PbCl_n^{2-n}$ (n = 1 … 4), which strongly increase the solubility of lead. A model for speciation in solutions of NaCl, KCl, $CaCl_2$, and $MgCl_2$ was developed for this purpose (Fig. 17).

In strongly alkaline solutions, these chloro complexes are replaced by hydrolysis species $Pb(OH)_n^{2-n}$ (n = 1 … 3). Important solubility-determining solid phases are $PbCl_2$ (cottunite), PbClOH (laurionite), $(PbO)_3{\cdot}PbCl_2{\cdot}H_2O$ (blixite), $PbSO_4$ (anglesite), and $K_2Pb(SO_4)_2$ (palmierite). Fig. 18 shows the experimental solubility of Pb(II) in solutions with pH_m 7.5 to 12.5, which is saturated with NaCl (halite) and anhydrite ($CaSO_4$). The deviation between experimental data and solubilities calculated with THEREDA at pH_m values above 10 can possibly be attributed to the formation of mixed chloro-hydroxo complexes, for which there is currently no model. Their formation is very well documented for Pd(II) (Rai et al., 2012), which is chemically similar to Pb(II) in many respects.

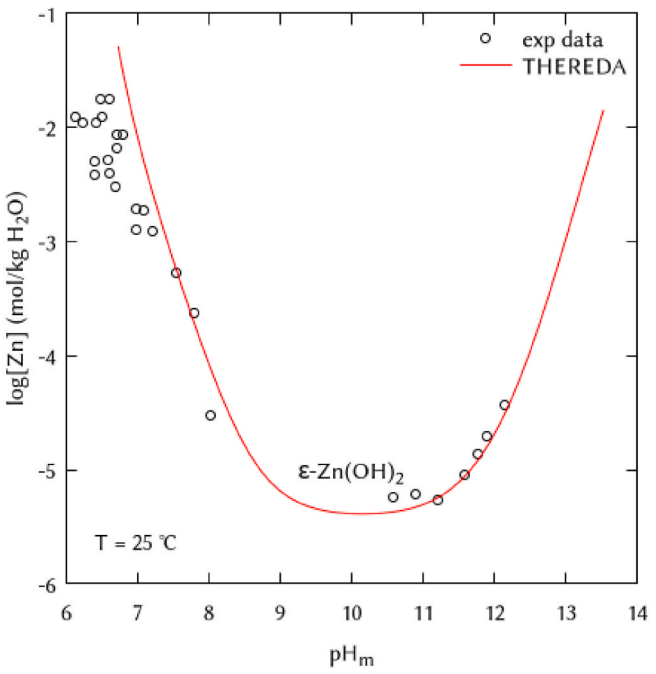

Fig. 19. Solubility of ε-$Zn(OH)_2$ as a function of pH, at I < 0,02 (NaOH) and 25 °C. Points: Experimental data from Fulton and Swinehart (1954). Lines: Calculation with THEREDA using PHREEQC Interactive version 3.8.6.17100 (Parkhurst and Appelo, 2013).

Carbonato and sulphato complexes play a relevant role in weakly mineralised solutions. $PbSO_4$ (anglesite), $PbCO_3$ (cerussite), $Pb_3(CO_3)_2(OH)_2$ (hydrocerussite), and possibly also phosphates such as $Pb_5(PO_4)_3OH$ (hydroxypyromorphite) then dominate as solid phases. For anglesite, systematic studies for its solubility exist and can be reproduced with THEREDA (no figure shown). This is not the case for the other phases mentioned, for which thermodynamic data were selected in THEREDA, but thus calculated solubilities should be regarded with caution (Moog, 2022).

3.3.2. Zinc

In natural systems, zinc only occurs in the oxidation state Zn(II). Like lead, it forms chloro complexes. In THEREDA, however, Zn^{2+} is described as a free ion in chloride-rich solutions because the previous data for the development of a Pitzer model for chloro-complexes was insufficient (Hagemann, 2024). Models for describing the stability of $ZnCl_x$ (x = 1–4) complexes exist, but these are constrained to NaCl solutions with trace concentrations of Zn (e.g. (Akinfiev and Tagirov, 2014)). Constraining the model to solutions with a maximum zinc concentration of 6 mol/kg, however, it was possible to achieve a satisfactory description of the properties of Zn^{2+} in solutions of the system Na-K-Mg-Ca-Cl-SO_4-H_2O at 25 °C.

Zn does not form solid phases in chloride-rich acidic to neutral solutions up to $c_{Zn} = 6$ mol/kg. In weakly mineralised water, $Zn(OH)_2$ (in various polymorphs), $ZnCO_3$ (smithsonite), or e.g. $Zn_5(CO_3)_2(OH)_6$ (hydrozincite) can occur. THEREDA also offers a complete data set for these compounds. As an example, Fig. 19 demonstrates the solubility of ε-$Zn(OH)_2$as a function of pH, though at low ionic strength (I < 0.2).

3.4. Cement systems

Cementitious materials are ubiquitous in the context of nuclear waste repositories in salt and in other host rocks as well (Ma et al., 2024; Mengel et al., 2012). They can be used for waste immobilisation, waste packages, plugs and seals, backfills, and tunnel support. Cements with salt aggregates (salt-concrete) of different compositions, are considered as sealing structures in salt rock disposal sites (e.g., the Asse mine and the Morsleben repository in Germany (Bracke, 2012; Henning et al., 2024; Mengel et al., 2012). Therefore, it is important to be able to model the stability and interaction of cementitious materials with highly concentrated aqueous solutions that result from the evaporitic host rock and the degradation of salt aggregate. This requires accurate and complete thermodynamic data for solids such as cement phases and secondary reaction products, and for the aqueous phase such as Si, Al aqueous species and their Pitzer parameters.

For the treatment of Sorel phases in THEREDA, please refer to chapter 3.1.2.

3.4.1. Thermodynamic data for cement phases

THEREDA was extended with the thermodynamic data of hydrated cement phases from CEMDATA (Lothenbach et al., 2019). The original reported solubility products (Lothenbach et al., 2019) based on aqueous data from the PSI/Nagra database (Thoenen et al., 2014) were recast in terms of THEREDA master species.

CEMDATA (Lothenbach et al., 2019) was selected as the source for state-of-the-art thermodynamic data for modelling hydrated Portland, calcium aluminate, calcium sulfoaluminate, and blended cements, as well as for alkali-activated materials. The database contains thermodynamic equilibrium data for modelling common cement hydrated phases calcium-silicate-hydrate (C-S-H), hydrated calcium aluminates Al_2O_3–Fe_2O_3-mono (AFm) and –tri (AFt) substituted phases, hydrogarnet, hydrotalcite, zeolites, and magnesium-silicate-hydrate (M-S-H) that are valid over temperatures ranging from 0 to at least 100 °C. The data were derived from critically assessed experimental data on the solubility of relevant phases obtained at low ionic strength (IS < 1) combined with additional measurements for solid solutions (Lothenbach et al., 2019) using the extended Debye-Hückel model of Helgeson et al. (1981). The standard thermodynamic data for modelling these pure hydrate phases and solid solutions in CEMDATA refer to the infinite dilution standard state and were combined with the Pitzer aqueous model within THEREDA. Potential inconsistencies due to different activity models should remain well within experimental uncertainty, as both models converge at low IS, and the data in CEMDATA are based solely on experiments conducted at low IS. The aqueous speciation model for the dominant species in equilibrium with cement hydrates showed agreement between the original aqueous model in CEMDATA and the Pitzer formalism in THEREDA (Miron, 2024). Standard thermodynamic data for these cement phases are available in the upcoming release of THEREDA together with an updated Pitzer model for Al and Si speciation.

3.4.2. Pitzer model for Al-Si speciation

The Si and Al aqueous speciation model and the Pitzer interaction parameters with ions from the oceanic salt system were revised in Miron (2024). The standard reference thermodynamic data of Si and Al aqueous species and solids quartz, gibbsite, and boehmite together with a consistent set of polythermal interaction parameters within the oceanic salt system (Al–Si)–Na–K–Mg–Ca–Cl–SO_4–CO_3–H_2O were derived based on experimental data from measurements done for a range of compositions and temperatures. To obtain a complete dataset, for relevant interactions, supplemental parameter values were estimated based on charge analogy (e.g. with carbonate ions), relationship with SIT parameters (Plyasunov et al., 1998), or other relations (Wesolowski, 1992). For aqueous silica species, polythermal coefficients for interaction parameters were obtained based on amorphous silica solubility, potentiometric, and osmotic coefficient measurements (Miron, 2024), see examples in Fig. 20 a and b. No data were available to derive the interactions of the silica hydrolysed species with potassium, so these were estimated. The Ca^{2+} and Mg^{2+} concentration in the cementitious systems pore solution was kept at millimolar values in equilibrium with C-S-H and M-S-H phases. The effect of Ca^{2+} and Mg^{2+} was accounted for by complexation with silicon. Supplemental data were derived for one

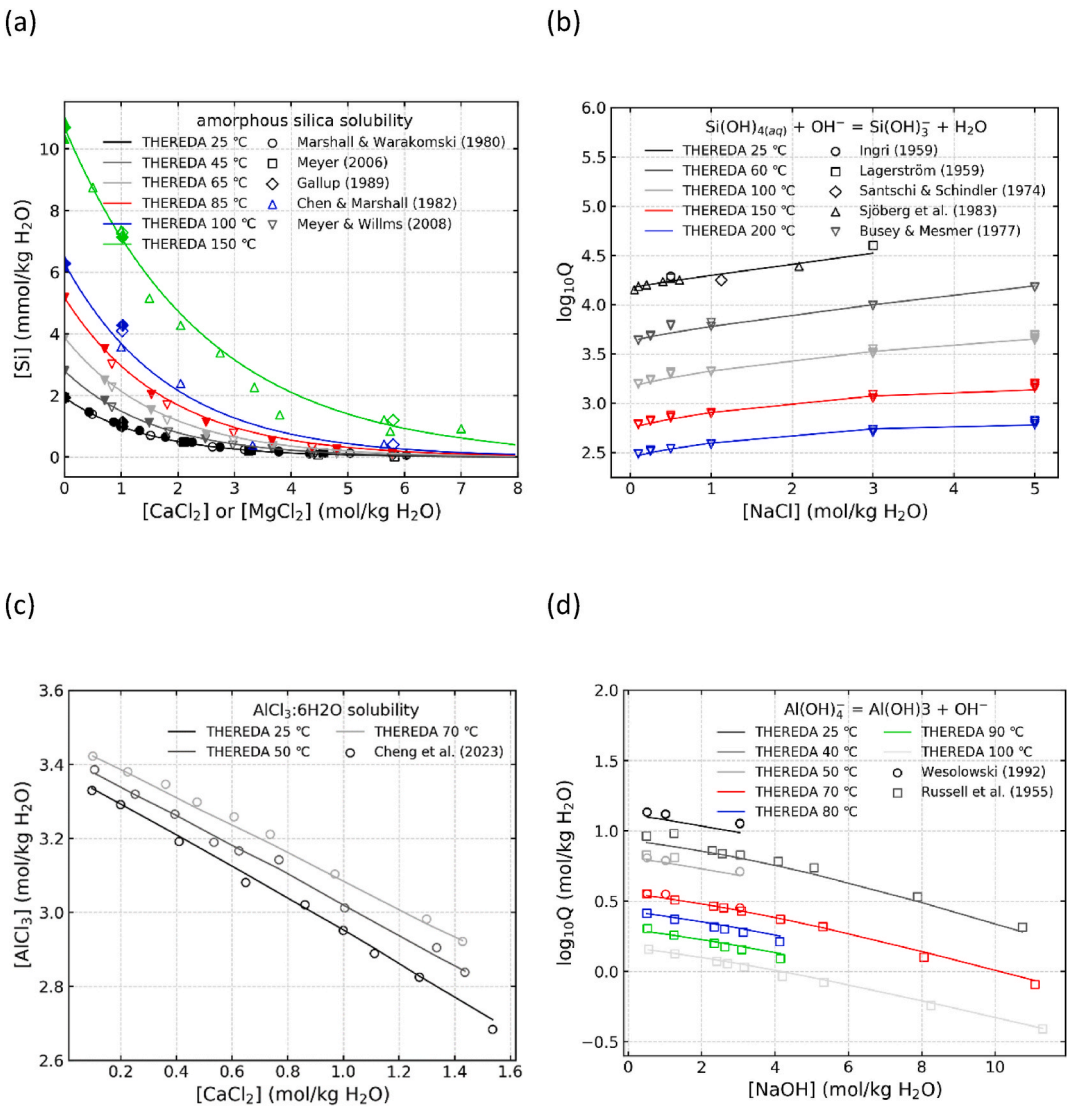

Fig. 20. (a) Solubility of amorphous silica in $MgCl_2$ (filled symbols) and $CaCl_2$ (empty symbols) solutions; (b) $Si(OH)_4(aq)$ first hydrolysis quotients in NaCl solution from potentiometric measurements; (c) $AlCl_3{\cdot}6H_2O$ solubility in $CaCl_2$ solutions; (d) gibbsite solubility quotient in NaOH solutions at different temperatures. Calculations using GEM-Selektor 3.9.6 (Busey and Mesmer, 1977; Chen and Marshall, 1982; Cheng et al., 2023; Gallup, 1989; Ingri, 1959; Kulik et al., 2013; Lagerström, 1959; Marshall and Warakomski, 1980; Meyer, 2006; Russell et al., 1955; Santschi and Schindler, 1974; Sjöberg et al., 1983; Wesolowski, 1992; Meyer and Willms, 2008).

silicon tetramer aqueous polymeric species, $Si_4O_8(OH)_4^{4-}$, which can be used to describe the solubility of SiO_2(am) at pH > 10 and < 0.1 mol·kg^{-1}. More detailed studies are required on silicon polymeric species stability and interactions with various electrolyte solutions as they can be relevant in later stages of cement degradation with pore solutions rich in silicon.

For aqueous aluminum species, revised standard thermodynamic data and interaction parameters with polythermal coefficients were mainly based on solubility measurements of $Al(OH)_3$ gibbsite, AlO(OH) boehmite, and $AlCl_3{\cdot}6H_2O$ (Fig. 20 c and d), complemented by osmotic coefficient data in various electrolyte solutions over a range of temperatures covering both low and high pH systems (see Miron (2024)). At high pH, relevant for cementitious systems, estimated interaction parameters with sulfate and carbonate ions reproduce available data on gibbsite solubility in Na_2CO_3 solutions (Königsberger et al., 2006), and in synthetic Bayer liquors (Bouzat and Philipponneau, 1991). Estimates for interactions between aluminum, calcium, and magnesium were difficult to assess due to their low concentration and solids precipitation at elevated pH. Potential Al-Si aqueous species interactions at high pH were assumed to be minimal as both are dominated by negatively charged species. The formation of Al-Si complexes was inconclusive and systems with zeolites in alkaline solutions were well reproduced (Xiong, 2013). Polymeric species become relevant in solutions where Si and Al are significantly above millimolar concentrations, which form in highly degraded cements and in alkali-activated systems. These are not currently well covered by THEREDA. Ordinary cementitious systems with common hydrate phases (silicate hydrates, AFm, AFt, hydrogarnet) were well described with monomeric Si and Al species and the updated Pitzer parameter dataset (Miron, 2024).

3.4.3. *Cement brine interaction*

When ordinary Portland cement materials, containing C-S-H, portlandite, ettringite, and AFm phases, interact with salt solutions, the type and concentration of salts can lead to significant changes in the composition of cement hydrate phases. These changes include leaching of calcium-rich phases, portlandite, AFm phases, and C-S-H phases, as well as dissolution of primary hydrates, and formation of secondary phases, often accompanied by changes in porosity (e.g., Xie et al. (2019);

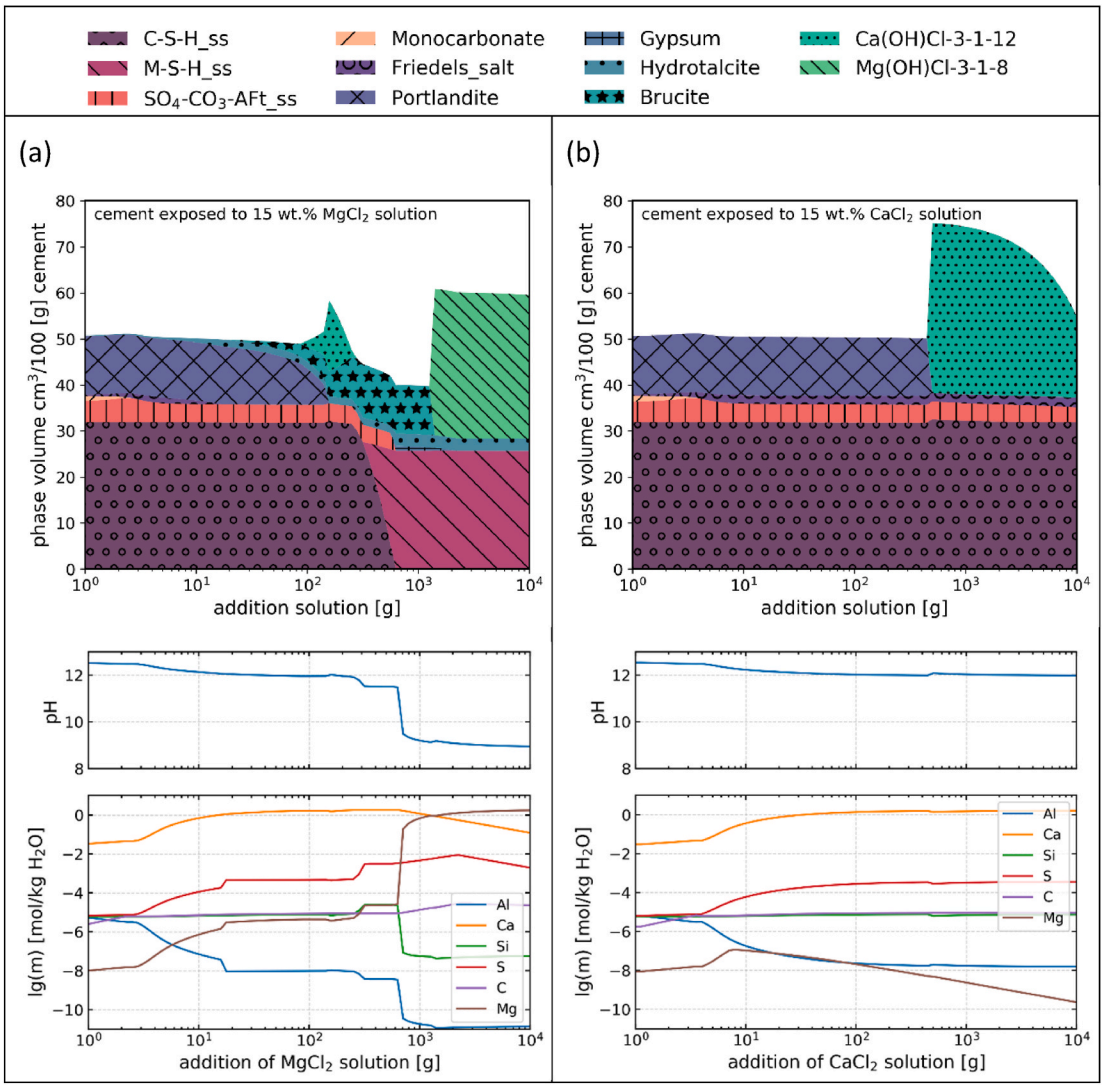

Fig. 21. Evolution of phases (top) and pore solution (bottom) of 100 g white Portland cement paste from Kulik et al. (2021) reacting with increasing amounts of (a) 1.85 mol/L $MgCl_2$ (15 wt%) and (b) 1.59 mol/L $CaCl_2$ (15 wt%) solutions. The C-S-H and M-S-H phases were calculated using an ideal solid solution model, and the SO_4-CO_3-AFt (ettringite) using a binary non-ideal model (Lothenbach et al., 2019) implemented in THEREDA. Calculations using GEM-Selektor 3.9.6 (Kulik et al., 2013).

De Weerdt et al. (2023); Li et al. (2024)). Such processes change the mechanical and hydrodynamical (or petrophysical) properties and contribute to the physicochemical deterioration of cement materials.

In the presence of chloride-rich solutions (e.g., NaCl, $MgCl_2$, $CaCl_2$), aluminate phases are replaced by layered double hydroxide (LDH) phases, such as Friedel's and Kuzel's salts. The calcium released from portlandite dissolution can further contribute to the formation of calcium hydroxide chloride hydrate phases. Magnesium-rich solutions promote the formation of secondary phases, such as magnesium hydroxide (brucite) and magnesium hydroxide chloride hydrates and induce the replacement of C-S-H by M-S-H gel. Aluminum released from aluminate phase dissolution, together with magnesium from the solution, can stabilise hydrotalcite-like Mg-Al-LDH phases (De Weerdt et al., 2023). With the inclusion of cement hydrate phases in THEREDA and the Pitzer formalisms, calculations involving interaction of cement with concentrated saline solutions can be performed in release 2025 (e.g., Fig. 21). Such calculations were not feasible with the original aqueous model in CEMDATA when dealing with multicomponent mixtures at high ionic strength. Fig. 21: presents a simplified calculation based on THEREDA, assuming an equilibrium bulk reaction, to illustrate the pore solution and phase assemblage evolution in a Portland cement paste exposed to progressively increasing amounts of $MgCl_2$ and $CaCl_2$ solutions. This calculation highlights the contrasting behaviors of the two solutions also observed in experiments (e.g., Xie et al. (2019); De Weerdt et al. (2023); Li et al. (2024)). In both cases, Friedel's salt $Ca_4Al_2Cl_2(OH)_{12}{\cdot}4H_2O$ was predicted to form, but only in case of $CaCl_2$ its formation appeared over the whole range of solution addition. Exposure to increasing amounts of $MgCl_2$ solution resulted in the complete replacement of all main cement hydrates, a drop in pH from 12.5 to 9, and the formation of new phases. In contrast, exposure to $CaCl_2$ primarily led to the dissolution of portlandite, a small pH decrease from 12.5 to 12.0, and the formation of calcium hydroxide chloride hydrates. The calculated evolution of the pore solution shows similar trends in elemental concentration for both cases. However, more pronounced changes occur when reacting with the $MgCl_2$ solution, as calcium and sulfur are released from the dissolution of all original cement phases and would be leached out in an open system. These calculations indicate the higher risks that $MgCl_2$-rich solutions pose to the integrity of Ca-based cement materials due to the leaching and dissolution of the Ca phases (in the case of Sorel cement, it would be resistant to $MgCl_2$-containing solutions, cf. Chapter 3.1.2).

4. Public access and use of THEREDA

Apart from application examples, which were already addressed in chapter 2.2, THEREDA features the following aspects.

4.1. Code-specific parameter files

The primary working product of THEREDA are parameter files for geochemical codes. The choice of supported codes always reflected the habits of members in the management board and is subject to change. At the beginning of THEREDA (2010), parameter files for PHREEQC (Parkhurst and Appelo, 2013), Geochemist's Workbench (Bethke, 2021), EQ3/6 (Wolery, 1992), and ChemApp (Eriksson et al., 1995, 1997) were issued. With the first cumulative release in 2020, EQ3/6 was abandoned and TOUGHREACT (Xu et al., 2011) added. In the latest release (2023a), only PHREEQC and Geochemist's Workbench were supported. At any time, all parameter files issued underwent testing.

Along with code-specific parameter files, data are additionally released in JSON-format (JavaScript Object Notation), offering programmers the possibility to import THEREDA-data into other codes. For more information about JSON, see http://json.org (accessed 2025-05-19).

4.2. Online data access

For registered users, released data can also be viewed on the THEREDA homepage. For registration, only name and email address are required. Not only the data included in the released parameter files are displayed, but also all data (dependent and independent) related to the species or solid phase of interest. References are given for independent data.

4.3. Documentation of data selection

THEREDA follows a different approach to other database projects where documents are provided about the selection of data in the entire database. In THEREDA, most of the data originate from individual publications and are referenced as such. Only in cases where this is not possible, a documentation of data selection is written and internally reviewed. These documents are available for the user in a dedicated section on the homepage of THEREDA.

Examples for this approach are the calculation of Debye-Hückel parameters, or thermodynamic standard functions for pure water. At the beginning of the project, all documentation for THEREDA was referred to as "Technical Paper". Recently, the creation of documentation about data selection in a different format called "THEREDA-Journal" was begun, while Technical Papers are reserved for purely technical details of THEREDA. When appropriate, data selection documentation is prepared as peer reviewed publications.

5. Outlook for THEREDA

In 2025, THEREDA will enter the 5th project phase. This will comprise a selection and prioritization of further chemical elements to be considered in THEREDA. Wherever possible, data gaps will be closed. Available thermodynamic data will be subject to critical review and stepwise integrated, with consistency in mind. Unavoidably, this is in part going to include data of less reliability than usual in the past project phases. But with quality flags assigned accordingly (see chapter 2.5), the user will be made aware of this fact. Future experimental work can focus on data that have the highest impact on computational results relevant for performance assessment.

Quantitatively, future extensions will be related mainly to chemotoxic heavy metals, actinides and Tc with inorganic ligands, as well as to actinides with organic ligands (citrate, EDTA, and gluconate). The next release of THEREDA will include CO_2 solubility, cadmium, and an update of the Tc selection. Further releases will include nitrate and the solubility of gases (H_2, CH_4, H_2S), including a Pitzer model for sulphide.

Parallel to these activities, efforts will be undertaken to integrate methods for the estimation of unknown data in the extension of THEREDA. Furthermore, it is planned to add the Paul Scherrer Institute to the management board and to add GEMS (Wagner et al., 2012; Kulik et al., 2013) to the suite of supported codes.

6. Summary

THEREDA is a thermodynamic database focusing on the calculation of solubilities in high saline solutions of relevance in the context of repositories for nuclear waste disposal in salt rock formations and other high ionic strength systems. For this purpose, equilibrium constants and Pitzer coefficients are selected and combined to form an internally consistent dataset. The term "selection" includes "adoption" from other sources if possible and "optimization" for the systems of interest if necessary. The core of THEREDA relies on the thermodynamic constants and Pitzer parameters selected for the system of oceanic salts, Na-K-Mg-Ca-Cl-SO_4-H_2O, which allow for the accurate description of the stability and mineral diagenesis of evaporites. This model is extended to account for the solubility of radionuclides, chemo-toxic elements, and other chemical elements with a potentially high impact on the geochemical milieu, as well as the stability of barrier materials. Besides chloride, sulfate, and hydroxide, thermodynamic data selection includes aqueous complexation and solubility processes involving carbonate and phosphate. Future releases of THEREDA will include nitrate and relevant organic ligands as well in the context of repositories for waste disposal.

Working procedures and supporting programmes are implemented to assist in checking the quality of released code-specific parameter files, in tracing back selected thermodynamic data and validation data, and in making all this information publicly available. The categorisation of thermodynamic data and Pitzer coefficients in terms of reliability and experimental origin offers the possibility to focus future research on the improvement of those with the highest impact on performance assessment. As the task of disposing of nuclear waste is going to be an effort for decades to come, the THEREDA project also represents a framework for the preservation of knowledge and competence.

CRediT authorship contribution statement

Helge C. Moog: Writing – review & editing, Writing – original draft, Supervision, Project administration, Funding acquisition, Conceptualization. **Marcus Altmaier:** Writing – review & editing. **Frank Bok:** Writing – original draft, Visualization. **Vinzenz Brendler:** Writing – review & editing. **Daniela Freyer:** Writing – review & editing, Writing – original draft. **Xavier Gaona:** Writing – review & editing, Writing – original draft. **Sven Hagemann:** Writing – original draft. **Claudia Joseph:** Writing – review & editing. **George-Dan Miron:** Writing – review & editing, Writing – original draft, Visualization. **Melanie Pannach:** Writing – review & editing, Writing – original draft, Visualization. **Julia Sohr:** Writing – review & editing, Writing – original draft, Visualization. **Wolfgang Voigt:** Writing – review & editing. **Marie Voss:** Writing – review & editing. **Laurin Wissmeier:** Writing – review & editing.

Declaration of competing interest

The authors declare that they have no known competing financial interests or personal relationships that could have appeared to influence the work reported in this paper.

Acknowledgement

Funding by the Bundesgesellschaft für Endlagerung (BGE), contract number 45181017, is acknowledged.

Data availability

References for all data used in THEREDA are accessible on our homepage www.thereda.de.

References

Akinfiev, N.N., Tagirov, B.R., 2014. Zn in hydrothermal systems: thermodynamic description of hydroxide, Chloride, and hydrosulfide complexes. Geochem. Int. 52, 197–214. https://doi.org/10.1134/S0016702914030021.

Altmaier, M., Brendler, V., Bube, C., Neck, V., Marquardt, C., Moog, H.C., Richter, A., Scharge, T., Voigt, W., Wilhelm, S., Willms, T., Wollmann, G., 2011. THEREDA - Thermodynamische Referenz-Datenbasis - Abschlussbericht (No. GRS-265).

Altmaier, M., Neck, V., Denecke, M.A., Yin, R., Fanghänel, T., 2006. Solubility of $ThO_2{\cdot}xH_2O$(am) and the Formation of ternary Th(IV) hydroxide-carbonate complexes in $NaHCO_3$-Na_2CO_3 solutions containing 0−4 M NaCl. Radiochim. Acta 94, 495–500. https://doi.org/10.1524/ract.2006.94.9-11.495.

Altmaier, M., Neck, V., Fanghänel, T., 2008. Solubility of Zr(IV), Th(IV) and Pu(IV) hydrous oxides in $CaCl_2$ solutions and the formation of ternary Ca-M(IV)-OH complexes. Radiochim. Acta 96, 541–550. https://doi.org/10.1524/ract.2008.1535.

Altmaier, M., Neck, V., Müller, R., Fanghänel, T., 2005. Solubility of $ThO_2{\cdot}xH_2O$(am) in carbonate solution and the formation of ternary Th(IV) hydroxide-carbonate complexes. Radiochim. Acta 93, 83–92.

Altmaier, M., Yalçıntaş, E., Gaona, X., Neck, V., Müller, R., Schlieker, M., Fanghänel, T., 2017. Solubility of U(VI) in chloride solutions. I. The stable Oxides/Hydroxides in NaCl systems, solubility products, hydrolysis constants and SIT coefficients. J. Chem. Therm. 114, 2–13. https://doi.org/10.1016/j.jct.2017.05.039.

Autenrieth, H., Braune, G., 1960. The stable and unstable regions of the reciprocal salt pairs NaCl + $MgSO_4$ + H_2O in the case of saturation with NaCl. Kali Steinsalz 3, 85–97.

Baumann, A., Yalcintas, E.P., Gaona, X., Altmaier, M., Geckeis, H., 2017. Solubility and hydrolysis of Tc(IV) in dilute to concentrated KCl solutions: an extended thermodynamic model for Tc^{4+}–H^+–K^+–Na^+–Mg^{2+}–Ca^{2+}–OH^-–Cl^-–H_2O(l) mixed systems. New J. Chem. 41, 9077–9086.

Benbow, S., Metcalfe, R., Wilson, J., 2008. Pitzer Databases for use in Thermodynamic modeling. Nuclear Waste Management Organization Technical Memorandum (QRS-3021A-TM1) Version 1.

Bertrams, N., Bollingerfehr, W., Eickemeier, R., Fahland, S., 2020a. RESUS-Grundlagen zur Bewertung eines Endlagersystems in steil lagernden Salzformationen. Gesellschaft für Anlagen-und Reaktorsicherheit (GRS) gGmbH. GRS-Report 569. ISBN 978-3-947685-55-4.

Bertrams, N., Bollingerfehr, W., Eickemeier, R., Fahland, S., Flügge, J., Frenzel, B., Hammer, J., Kindlein, J., Liu, W., Maßmann, J., Mayer, K., Mönig, J., Mrugalla, S., Müller-Hoeppe, N., Reinhold, K., Rübel, A., Schubarth-Engelschall, N., Simo, E., Thiedau, J., Wolf, J., 2020b. RESUS Grundlagen zur Bewertung eines Endlagersystems in flach lagernden Salzformationen. Gesellschaft für Anlagen-und Reaktorsicherheit (GRS) gGmbH. GRS-Report 568. ISBN 978-3-947685-54-7.

Bethke, C.M., 2021. Geochemical and Biogeochemical Reaction Modeling, third ed. Cambridge University Press, Cambridge.

Bischofer, B., Hagemann, S., Altmaier, M., Banik, N., Bosbach, D., Bracke, G., Brendler, V., Curtius, H., Finck, N., Franzen, C., Gaona, X., Geckeis, H., Heberling, F., Herm, M., Kindlein, J., Marsac, R., Metz, V., Muñoz, A., Rozov, K., Yalcintas, E., 2016. Behaviour of Long-Lived Fission and Activation Products in the Nearfield of a Nuclear Waste Repository and the Possibilities of their Retention.

Bok, F., 2021. Thermodynamic Model for the Systems Se(+Vi,+Iv) – Na, K, Mg, Ca – Cl, SO_4, CO_3 – H_2O at T = 0–100 °C. HZDR (Technical Report No. Revision 1.0 as of 2021-12-02).

Bornemann, O., Behlau, J., Fischbek, R., Hammer, J., Jaritz, W., Keller, S., Mingerzahn, G., Schramm, M. (Eds.), 2008. Standortbeschreibung Gorleben Teil 3. Schweizerbart Science Publishers, Stuttgart, Germany.

Bornemann, O., Fischbeck, R., 1987. Display of Cores in the Bundesanstalt für Geowissenschaften und Rohstoffe 3000 Hannover - zechstein 2-4 des Salzstocks Gorleben. Presented at the Exkursionsführer I, Internationales Symposium Kassel - Hannover, pp. 145–160.

Bouzat, G., Philipponneau, G., 1991. Physical chemistry models of oxalate and gibbsite solubilities in Bayer solutions. Light Met. 97–102.

Bracke, G., 2012. Aspects of final disposal of radioactive waste in Germany. Turk. J. Earth Sci. 21, 145. https://doi.org/10.3906/yer-1006-18.

Brönsted, J.N., 1922a. Studies on solubility. IV. The principle of the specific interaction of ions. J. Am. Chem. Soc. 44, 877–898. https://doi.org/10.1021/ja01426a001.

Brönsted, J.N., 1922b. Calculation of the osmotic and activity functions in solutions of uni-univalent salts. J. Am. Chem. Soc. 44, 938–948. https://doi.org/10.1021/ja01426a003.

Busey, R.H., Holmes, H.F., Mesmer, R.E., 1984. The enthalpy of dilution of aqueous sodium chloride to 673 K using a new heat-flow and liquid-flow microcalorimeter. Excess thermodynamic properties and their pressure coefficients. J. Chem. Therm. 16, 343–372. https://doi.org/10.1016/0021-9614(84)90174-5.

Busey, R.H., Mesmer, R.E., 1977. Ionization equilibriums of Silicic Acid and polysilicate Formation in aqueous sodium chloride solutions to 300 degree C. Inorg. Chem. 16, 2444–2450. https://doi.org/10.1021/ic50176a004.

Campbell, A.N., Downes, K.W., Samis, C.S., 1934. The system $MgCl_2$—KCl—$MgSO_4$—K_2SO_4—H_2O at 100°. J. Am. Chem. Soc. 56, 2507–2512.

Chen, C.-T.A., Marshall, W.L., 1982. Amorphous Silica solubilities IV. Behavior in pure water and aqueous sodium chloride, sodium sulfate, magnesium chloride, and magnesium sulfate solutions up to 350°C. Geochem. Cosmochim. Acta 46, 279–287. https://doi.org/10.1016/0016-7037(82)90255-1.

Cheng, W., Li, J., Xu, L., Cheng, F., Liu, G., 2023. Experiment and prediction for the solubility of $AlCl_3{\cdot}6H_2O$ in $FeCl_3$, $CaCl_2$, KCl and KCl-$FeCl_3$ solutions. Huagong Xuebao/CIESC J. 74, 642–652. https://doi.org/10.11949/0438-1157.20221368.

Christov, C., Møller, N., 2004a. Chemical equilibrium model of solution behavior and solubility in the H-Na-K-OH-Cl-HSO_4-SO_4-H_2O system to high concentration and temperature. Geochem. Cosmochim. Acta 68, 1309–1331. https://doi.org/10.1016/j.gca.2003.08.017.

Christov, C., Møller, N., 2004b. A chemical equilibrium model of solution behavior and solubility in the H-Na-K-Ca-OH-Cl-HSO_4-SO_4-H_2O system to high concentration and temperature. Geochem. Cosmochim. Acta 68, 3717–3739. https://doi.org/10.1016/j.gca.2004.03.006.

D'Ans, J., Busse, W., Freund, H., 1955. Über basische Magnesiumchloride (Basic magnesium chloride). Kali Steinsalz 8, 3–7.

De Weerdt, K., Bernard, E., Kunther, W., Pedersen, M.T., Lothenbach, B., 2023. Phase changes in cementitious materials exposed to saline solutions. Cement Concr. Res. 165, 107071. https://doi.org/10.1016/j.cemconres.2022.107071.

Debure, M., Lassin, A., Marty, N.C., Claret, F., Virgone, A., Calassou, S., Gaucher, E.C., 2019. Thermodynamic evidence of giant salt deposit formation by serpentinization: an alternative mechanism to solar evaporation. Sci. Rep. 9, 11720. https://doi.org/10.1038/s41598-019-48138-9.

Eriksen, T., Ndalamba, P.I., Bruno, J., Caceci, M., 1992. The solubility of $TcO_2 \cdot nH_2O$ in neutral to alkaline solutions under constant pco_2. Radiochim. Acta 58–59. https://doi.org/10.1524/ract.1992.5859.1.67.

Eriksson, G., Hack, K., Petersen, S., 1997. ChemApp – a programmable thermodynamic calculation interface. Werkstoffwoche '96, Symposium 8 Simulation, Modellierung, Informationssysteme 47. Presented at the Werkstoffwoche '96, DGM Informationsgesellschaft mbH, Hamburger Allee 26, D-60486 Frankfurt, Germany.

Eriksson, G., Spencer, P.J., Sippola, H., 1995. A general thermodynamic software interface. In: Jokilaakso, A. (Ed.), Proceedings of the 2nd Colloquium on Process Simulation. Presented at the 2nd Colloquium on Process Simulation, p. 113. Espoo, Finnland.

Eugster, H.P., Harvie, C.E., Weare, J.H., 1980. Mineral equilibria in a six-component seawater system, Na-K-Mg-Ca-SO_4-Cl-H_2O, at 25°C. Geochem. Cosmochim. Acta 44, 1335–1347. https://doi.org/10.1016/0016-7037(80)90093-9.

Fellhauer, D., Altmaier, M., Gaona, X., Lützenkirchen, J., Fanghänel, T., 2016a. Np(V) solubility, speciation and solid phase formation in alkaline $CaCl_2$ solutions. Part II: thermodynamics and implications for source term estimations of nuclear waste disposal. Radiochim. Acta 104, 381–397. https://doi.org/10.1515/ract-2015-2490.

Fellhauer, D., Rothe, J., Altmaier, M., Neck, V., Runke, J., Wiss, T., Fanghänel, T., 2016b. Np(V) solubility, speciation and solid phase formation in alkaline $CaCl_2$ solutions. Part I: experimental results. Radiochim. Acta 104. https://doi.org/10.1515/ract-2015-2489, 25-S.

Frowein, F., Von Mühlendahl, E., 1926. Die Lösungen des Doppelt-Ternären Salzgemisches (K_2/Mg/Na_2)((NO_3)$_2$/Cl_2) und Ihre Bedeutung für die Technik. Angew. Chem. 39, 1488–1500. https://doi.org/10.1002/ange.19260394804.

Fulton, J.W., Swinehart, D.F., 1954. The equilibria of Crystalline zinc hydroxide in Dilute Hydrochloric acid and sodium hydroxide at 25°. The first and second acidic dissociation constants of zinc Hydroxide1,2. J. Am. Chem. Soc. 76, 864–867. https://doi.org/10.1021/ja01632a068.

Gallup, D., 1989. Solubility of Amorphous Silica in geothermal brines. Transac. Geotherm. Resourc. Council 13, 241–245.

Giffaut, E., Grivé, M., Blanc, Ph, Vieillard, Ph, Colàs, E., Gailhanou, H., Gaboreau, S., Marty, N., Madé, B., Duro, L., 2014. Andra thermodynamic database for performance assessment: thermochimie. Appl. Geochem. 49, 225–236. https://doi.org/10.1016/j.apgeochem.2014.05.007.

Goodwin, D., Moffat, H., Speth, R., 2015. Cantera: an object-oriented Software Toolkit for Chemical Kinetics, Thermodynamics, and Transport Processes. Version 2.2.0.

Greenberg, J.P., Møller, N., 1989. The prediction of mineral solubilities in natural waters: a chemical equilibrium model for the Na-K-Ca-Cl-SO_4-H_2O System to high concentration from 0 to 250°C. Geochem. Cosmochim. Acta 53, 2503–2518. https://doi.org/10.1016/0016-7037(89)90124-5.

Grenthe, I., Gaona, X., Plyasunov, A.V., Rao, L., Runde, W.H., Grambow, B., Konings, R.J.M., Smith, A.L., Moore, E.E., 2020. Second update on the chemical thermodynamics of uranium, neptunium, plutonium, americium and technetium. Nuclear Energy Agency of the OECD (NEA).

Grivé, M., Duro, L., Colàs, E., Giffaut, E., 2015. Thermodynamic data selection applied to radionuclides and chemotoxic elements: an overview of the ThermoChimie-TDB. Appl. Geochem. 55, 85–94. https://doi.org/10.1016/j.apgeochem.2014.12.017.

Guggenheim, E.A., 1966. Applications of Statistical Mechanics.

Hagemann, S., 2024. Development of a thermodynamic model for zinc, lead and cadmium in saline solutions (No. GRS-653). Gesellschaft für Anlagen-und Reaktorsicherheit (GRS) gGmbH.

Hagemann, S., 1999. *Thermodynamische Eigenschaften des Bleis in Lösungen der ozeanischen Salze.* Doctoral dissertation. TU Braunschweig, Germany.

Harvie, C.E., Møller, N., Weare, J.H., 1984. The prediction of mineral solubilities in natural waters: the Na-K-Mg-Ca-H-Cl-SO_4-OH-HCO_3-CO_3-CO_2-H_2O System to high ionic strengths at 25°C. Geochem. Cosmochim. Acta 48, 723–751. https://doi.org/10.1016/0016-7037(84)90098-X.

Haynes, Henry Jr., W., 1997. Solution mining of trona. *In.* Situ 21 (4), 357–394.

Helgeson, H.C., Kirkham, D.H., Flowers, G.C., 1981. Theoretical prediction of the thermodynamic behavior of aqueous electrolytes by high pressures and temperatures; IV, calculation of activity coefficients, osmotic coefficients, and apparent molal and standard and relative partial molal properties to 600 degrees C and 5kb. Am. J. Sci. 281, 1249–1516.

Henning, R., Sturm, P., Keßler, S., Gluth, G.J.G., 2024. Influence of salt aggregate on the degradation of Hybrid Alkaline Cement (HAC) concretes in Magnesium Chloride-Rich saline solution simulating evaporite rock. Appl. Geochem. 168, 106027. https://doi.org/10.1016/j.apgeochem.2024.106027.

Holmes, H.F., Baes, C.F., Mesmer, R.E., 1981. Isopiestic Studies of Aqueous Solutions at Elevated Temperatures III. {(1 −y)NaCl + yCaCl$_2$}. J. Chem. Therm. 13, 101–113. https://doi.org/10.1016/S0021-9614(81)80015-8.

Holmes, H.F., Baes, C.F., Mesmer, R.E., 1979. Isopiestic studies of aqueous solutions at elevated temperatures II. NaCl + KCl mixtures. J. Chem. Therm. 11, 1035–1050. https://doi.org/10.1016/0021-9614(79)90134-4.

Holmes, H.F., Baes, C.F., Mesmer, R.E., 1978. Isopiestic studies of aqueous solutions at elevated temperatures I. KCl, CaCl$_2$, and MgCl$_2$. J. Chem. Therm. 10, 983–996. https://doi.org/10.1016/0021-9614(78)90060-5.

Holmes, H.F., Mesmer, R.E., 1996. Aqueous solutions of the alkaline-earth metal chlorides at elevated temperatures. Isopiestic molalities and thermodynamic properties. J. Chem. Therm. 28, 1325–1358. https://doi.org/10.1006/jcht.1996.0117.

Holmes, H.F., Mesmer, R.E., 1994. An Isopiestic Study of {(1 - y)NaHSO$_4$ + yNa$_2$SO$_4$}(aq) at Elevated Temperatures. J. Chem. Therm. 26, 581–594. https://doi.org/10.1006/jcht.1994.1067.

Holmes, H.F., Mesmer, R.E., 1986. Thermodynamics of aqueous solutions of the alkali metal sulfates. J. Solut. Chem. 15, 495–517. https://doi.org/10.1007/BF00644892.

Holmes, H.F., Mesmer, R.E., 1983. Thermodynamic properties of aqueous solutions of the alkali metal chlorides to 250°C. J. Phys. Chem. 87, 1242–1255. https://doi.org/10.1021/j100230a030.

Hovland, M., Rueslåtten, H., Johnsen, H.K., 2018. Large salt accumulations as a consequence of hydrothermal processes associated with 'Wilson cycles': a review, part 2: application of a new salt-forming model on selected cases. Mar. Petrol. Geol. 92, 128–148. https://doi.org/10.1016/j.marpetgeo.2018.02.015.

Hummel, W., Berner, U., Curti, E., Pearson, F., Thoenen, T., 2002. Nagra/PSI Chemical Thermodynamic Data Base 01/01.

Hummel, W., Thoenen, T., 2023. The PSI Chemical Thermodynamic Database 2020 (Nagra Technical Report No. NTB 21-03).

Igelsrud, I., Thompson, T.G., 1936. Equilibria in the saturated solutions of salts occurring in Sea water. II. The Quaternary System MgCl$_2$-CaCl$_2$-KCl-H$_2$O at 0°. J. Am. Chem. Soc. 58, 2003–2009. https://doi.org/10.1021/ja01301a053.

Ingri, N., 1959. Equilibrium studies of polyanions. Acta Chem. Scand. 13, 758–775. https://doi.org/10.3891/ACTA.CHEM.SCAND.13-0758.

Jang, J.J.-H., Nemer, M., 2016. Solubility model for ferrous iron hydroxide in sodium Chloride solutions spike with sodium EDTA: a pitzer approach. In: Report Number: SAND2016-8020C. Research Org. Sandia National Lab. (SNL-NM), Albuquerque, NM (United States).

Keitel, H., 1923. The systems KCl–MgCl$_2$–H$_2$O and NaCl–MgCl$_2$–H$_2$O. Kali 17, 248–251.

Keller, S., 2007. Langzeitsicherheitsanalyse für ein HAW-Endlager im Salz. Geologisches Referenzmodell Für Einen HAW-Endlagerstandort Im Salz (Technischer Bericht). BGR.

Khaidukov, N., Linetzkaya, Z., 1935. The water-vapor pressure above the solutions NaCl–KCl–MgCl$_2$–H$_2$O. Kali 8, 28–33.

Kiefer, C., Fellhauer, D., Altmaier, M., Gaona, X., 2025. Updated pitzer activity model for Tc(IV) solubility and hydrolysis in the Tc(IV)–Na$^+$–K$^+$–Ca^{2+}–Mg^{2+}–H$^+$–Cl$^-$–OH$^-$–H$_2$O(l) system. In: Preparation.

Kobayashi, T., Fellhauer, D., Sasaki, T., 2021. Solubility of PuO$_2$(am,hyd) and the formation of Pu(IV) Carbonate Complexes in Carbonate Solutions containing 0.1–5.0 mol·dm NaNO$_3$. J. Solut. Chem. 50, 1–15. https://doi.org/10.1007/s10953-021-01080-9.

Königsberger, E., May, P.M., Hefter, G., 2006. Comprehensive model of synthetic bayer liquors. Part 3. Sodium aluminate solutions and the solubility of gibbsite and boehmite. Monatsh. Chem./Chem. Mon. 137, 1139–1149. https://doi.org/10.1007/s00706-006-0526-9.

Krumgalz, B.S., 2017. Temperature dependence of mineral solubility in water. Part I. Alkaline and alkaline Earth chlorides. J. Phys. Chem. Ref. Data 46, 043101. https://doi.org/10.1063/1.5006028.

Kulik, D.A., Wagner, T., Dmytrieva, S.V., Kosakowski, G., Hingerl, F.F., Chudnenko, K.V., Berner, U.R., 2013. GEM-Selektor geochemical modeling package: revised Algorithm and GEMS3K Numerical Kernel for coupled simulation codes. Comput. Geosci. 17, 1–24. https://doi.org/10.1007/s10596-012-9310-6.

Kulik, D.A., Winnefeld, F., Kulik, A.K., Miron, G.D., Lothenbach, B., 2021. CemGEMS – an easy-to-use web application for thermodynamic modeling of cementitious materials. RILEM Technical Lett.

Kurnakov, N.S., Manoev, D.P., Osokoreva, N.A., 1932. Solubility of the carnallite system. Kali 2, 25.

Kurnakov, N.S., Opuchtina, M.A., 1930. Izvestiya instituta Fiziko-Khimicheskogo analiza. Akademiya Nauk SSSR 2.

Kurnakov, N.S., Osokoreva, N.A., 1935. Equilibrium of water solutions of potassium, sodium and magnesium chlorides at temperatures 10–110° C. Solikamskiye Karnallity, pp. 49–65.

Kurnakov, N.S., Žemčužny, S.F., 1924. Die Gleichgewichte des Reziproken Systems Natriumchlorid-magnesiumsulfat mit Berücksichtigung der Natürlichen Salzsolen. Z. Anorg. Allg. Chem. 140, 149–182. https://doi.org/10.1002/zaac.19241400111.

Lagerström, G., 1959. Equilibrium studies of polyanions. III. Silicate ions in NaClO$_4$ medium. Acta Chem. Scand. 13, 722–736. https://doi.org/10.3891/ACTA.CHEM.SCAND.13-0722.

Lee, W.B., Egerton, A.C., 1923. LXXXIII.—Heterogeneous equilibria between the chlorides of calcium, magnesium, potassium, and their aqueous solutions. Part I. J. Chem. Soc. Trans. 123, 706–716. https://doi.org/10.1039/CT9232300706.

Li, T., Chen, H., Zhang, T., Liu, L., Zheng, Y., 2024. Thermodynamic study on phase composition of hardened Portland cement paste exposed to CaCl$_2$ solution: effects of temperature, CaCl$_2$ concentration, and type and dosage of supplementary cementitious materials. Cement Concr. Res. 178, 107437. https://doi.org/10.1016/j.cemconres.2024.107437.

Lightfoot, W.J., Prutton, C.F., 1947. Equilibria in saturated salt solutions. II. The ternary systems CaCl$_2$-MgCl$_2$-H$_2$O, CaCl$_2$-KCl-H$_2$O and MgCl$_2$-KCl-H$_2$O at 75°. J. Am. Chem. Soc. 69, 2098–2100. https://doi.org/10.1021/ja01201a005.

Linke, W.F., Seidell, A., 1958. Solubilities: Inorganic and Metal-Organic Compounds: a Compilation of Solubility Data from the Periodical Literature.

Liu, D., Yao, J., Wang, B., Bruggeman, C., Maes, N., 2007. Solubility study of Tc(IV) in a granitic water. Radiochim. Acta 95, 523–528. https://doi.org/10.1524/ract.2007.95.9.523.

Lothenbach, B., Kulik, D.A., Matschei, T., Balonis, M., Baquerizo, L., Dilnesa, B., Miron, G.D., Myers, R.J., 2019. Cemdata18: a chemical thermodynamic database for hydrated Portland cements and alkali-activated materials. Cement Concr. Res. 115, 472–506. https://doi.org/10.1016/j.cemconres.2018.04.018.

Ma, B., Provis, J.L., Wang, D., Kosakowski, G., 2024. The essential role of cement-based materials in a radioactive waste repository. npj Mater. Sustain. 2, 21. https://doi.org/10.1038/s44296-024-00025-9.

Madé, B., Bower, W., Brassinnes, S., Colàs, E., Duro, L., Blanc, P., Lassin, A., Harvey, L., Begg, J.D., 2025. Recent developments in ThermoChimie – a thermodynamic database used in radioactive waste management. Appl. Geochem. 180. https://doi.org/10.1016/j.apgeochem.2024.106273.

Majima, K., Katsuki, K., Tejima, M., Oka, S., 1974. Equilibria of Quaternary systems NaCl-KCl-MgCl$_2$-H$_2$O and NaCl-KCl-CaCl$_2$-H$_2$O at 75°C. Bulletin of the Society of Sea Water Science, Japan 27, 315–320. https://doi.org/10.11457/swsj1965.27.315.

Majima, K., Katsuki, K., Tejima, M., Oka, S., 1972. Equilibrium of ternary system KCl-MgCl$_2$-H$_2$O, Quaternary systems NaCl-KCl-MgCl$_2$-H$_2$O and KCl-MgCl$_2$-CaCl$_2$-H$_2$O at 50°C. Bulletin of the Society of Sea Water Science, Japan 26, 199–204. https://doi.org/10.11457/swsj1965.26.199.

Marion, G.M., Kargel, J.S., 2008. Cold aqueous planetary geochemistry with FREZCHEM. Advances in Astrobiology and Biogeophysics, first ed. Springer, Berlin Heidelberg.

Marshall, W.L., Warakomski, J.M., 1980. Amorphous silica Solubilities—Ii. Effect of aqueous salt solutions at 25°C. Geochem. Cosmochim. Acta 44, 915–924. https://doi.org/10.1016/0016-7037(80)90281-1.

Mengel, K., Röhlig, K.-J., Geckeis, H., 2012. Endlagerung radioaktiver abfälle. Chem. Unserer Zeit 46, 208–217. https://doi.org/10.1002/ciuz.201200582.

Meyer, Th, 2006. Geochemische Modellierung des Langzeitverhaltens von Silikatischen und Alumosilikatischen Materialien. GRS-Report A-3350. Gesellschaft für Anlagen- und Reaktorsicherheit (GRS) mbH, Braunschweig, Germany.

Meyer, Th, Willms, Th, 2008. Geochemische Modellierung des Langzeitverhaltens von Silikatischen und Alumosilikatischen Materialien im Temperaturbereich bis 90°C. GRS-Report A-3493. Gesellschaft für Anlagen- und Reaktorsicherheit (GRS) mbH, Braunschweig, Germany.

Miron, G., 2024. Si–Al Pitzer Dataset: consistent Set of Pitzer Activity Model Interaction Parameters of Al and Si Species, for Modelling Cements in Saline Systems with THEREDA. https://doi.org/10.26434/chemrxiv-2024-m02f1-v2.

Moffat, H., Jové-Colón, C.F., 2009. Implementation of Equilibrium Aqueous Speciation and Solubility (EQ3 Type) Calculations into Cantera for Electrolyte Solutions.

Moog, H., 2022. Thermodynamic Database for Pb and its Compounds - Data Selection. THEREDA Journal. https://nbn-resolving.org/urn:nbn:de:bsz:105-qucosa2-802332.

Moog, H.C., Bok, F., Marquardt, C.M., Brendler, V., 2015. Disposal of nuclear waste in host rock formations featuring high-saline solutions – implementation of a thermodynamic reference database (THEREDA). Appl. Geochem. 55, 72–84. https://doi.org/10.1016/j.apgeochem.2014.12.016.

Motoyama, M.H., Kadota, M., Oka, S., 1976. Equilibrium in the quinary system NaCl-KCl-MgCl$_2$-CaCl$_2$-H$_2$O at 100°C. Bulletin of the Society of Sea Water Science, Japan 30, 26–34.

Nakayama, M., 1960. A new basic triple salt containing magnesium hydroxide. Bull. Agric. Chem. Soc. Jpn. 24, 362–371. https://doi.org/10.1271/bbb1924.24.362.

Nakayama, M., 1959. A new basic triple salt containing magnesium hydroxide: part II. The Quaternary system KCl-MgCl$_2$-Mg(OH)$_2$-H$_2$O at 100°. Bull. Agric. Chem. Soc. Jpn. 23, 46–48. https://doi.org/10.1080/03758397.1959.10857524.

Nikolaev, V.I., Burovaya, E.E., 1938. Surface tension and viscosity in the reciprocal system sodium chloride-magnesium sulfate. Izvestiya Sektora Fiziko-Khimicheskogo Analiza, Akademiya Nauk SSSR 10, 245–258.

Olin, Å., Noläng, B.I., Öhman, L., Osadchii, E.G., Rosén, E., 2005. Chemical Thermodynamics of Selenium.

Orlova, V.T., Yanat'eva, O.K., 1963. Zhurnal neorganicheskoi khimii. Zh. Neorg. Khim. 8, 1791ff.

Pabalan, R.T., Pitzer, K.S., 1988a. Heat capacity and other thermodynamic properties of Na2SO4(aq) in hydrothermal solutions and the solubilities of sodium sulfate minerals in the system Na-Cl-SO$_4$-OH-H$_2$O to 300°C. Geochem. Cosmochim. Acta 52, 2393–2404. https://doi.org/10.1016/0016-7037(88)90296-7.

Pabalan, R.T., Pitzer, K.S., 1988b. Apparent molar heat capacity and other thermodynamic properties of aqueous potassium chloride solutions to high temperatures and pressures. J. Chem. Eng. Data 33, 354–362. https://doi.org/10.1021/je00053a037.

Pabalan, R.T., Pitzer, K.S., 1987. Thermodynamics of concentrated electrolyte mixtures and the prediction of mineral solubilities to high temperatures for mixtures in the system Na-K-Mg-Cl-SO$_4$-OH-H$_2$O. Geochem. Cosmochim. Acta 51, 2429–2443. https://doi.org/10.1016/0016-7037(87)90295-X.

Palkin, A.P., 1935. Solubility study in the system KCl-NaCl-MgCl$_2$-H$_2$O at temperatures below 10°. Solikamskii Karnallity, pp. 66–87.

Palkin, A.P., Varasova, E.N., 1932. Solubilities in the systems: potassium chloride-sodium chloride-magnesium chloride-water at 0°C. Zhurnal Pikladnoi Khimii 5, 316–324.
Pannach, M., Bette, S., Freyer, D., 2017. Solubility Equilibria in the system Mg $(OH)_2$–$MgCl_2$–H_2O from 298 to 393. K. J. Chem. Eng. Data 62, 1384–1396. https://doi.org/10.1021/acs.jced.6b00928.
Pannach, M., Paschke, I., Metz, V., Altmaier, M., Voigt, W., Freyer, D., 2023. Solid-Liquid equilibria of sorel phases and Mg $(OH)_2$ in the System Na-Mg-Cl-OH-H_2O. Part I: experimental determination of OH^- and H^+ equilibrium concentrations and solubility constants at 25°C, 40°C, and 60°C. Front. Nuclear Eng. 2. https://doi.org/10.3389/fnuen.2023.1188789. Art.-Nr.
Parkhurst, D.L., Appelo, C.A.J., 2013. Description of input and examples for PHREEQC Version 3—A computer program for speciation, Batch-reaction, one-dimensional transport, and inverse geochemical calculations. In: U.S. Geological Survey Techniques and Methods, Book 6, Chap. A43. U.S. Geological Survey Techniques and Methods, p. 497ff.
Pel'sh, A., 1973. Reference Book of Experimental Data of the Solubility of Multicomponent Aqueous-Salt Systems.
Pel'sh, A., 1953. A square diagram for presentation of a quinary reciprocal system Na-K-Mg-Cl-SO_4 + H_2O. In: Trudy Vsesoyuz. Nauch.-Issledovatel. Inst. Galurgii., pp. 84–112
Phutela, R.C., Pitzer, K.S., Saluja, P.P.S., 1987. Thermodynamics of aqueous magnesium chloride, calcium chloride, and Strontium chloride at elevated temperatures. J. Chem. Eng. Data 32, 76–80. https://doi.org/10.1021/je00047a022.
Pitzer, K.S., 1991. Ion interaction approach: theory and data correlation. In: Activity Coefficients in Electrolyte Solutions. CRC Press, pp. 75–153.
Pitzer, K.S., Das, B., 1998. Thermodynamic properties of Na_2SO_4(aq) above 200°C. Geochem. Cosmochim. Acta 62, 915–916. https://doi.org/10.1016/S0016-7037(97)00380-3.
Plyasunov, A.V., Fanghänel, T., Grenthe, I., Salaneck, W.R., Sillanpää, R., Bernáth, G., Szúnyog, J., Långström, B., 1998. Estimation of the Pitzer Equation Parameters for Aqueous Complexes. A case study for Uranium at 298.15 K and 1 atm. Acta Chem. Scand. 52, 250–260.
Precht, H., Wittjen, B., 1881. Löslichkeit von Salzgemischen der Salze der Alkalien und alkalischen Erden bei verschiedener Temperatur. Ber. Dtsch. Chem. Ges. 14, 1667–1675. https://doi.org/10.1002/cber.18810140225.
Ragoussi, M., Brassinnes, S., 2015. The NEA thermochemical database Project:30 years of accomplishments. Radiochim. Acta 103, 679–685.
Ragoussi, M.-E., Costa, D., 2019. Fundamentals of the NEA thermochemical database and its influence over national nuclear programs on the performance assessment of deep geological repositories. J. Environ. Radioact. 196, 225–231. https://doi.org/10.1016/j.jenvrad.2017.02.019.
Rai, D., Felmy, A.R., Stemer, S.M., Moore, D.A., Mason, M.J., Novak, C.F., 1997. The solubility of Th(IV) and U(IV) hydrous oxides in concentrated NaCl and $MgCl_2$ solutions. Radiochim. Acta 79, 239–248. https://doi.org/10.1524/ract.1997.79.4.239.
Rai, D., Hess, N.J., Felmy, A.R., Moore, D.A., Yui, M., Vitorge, P., 1999. A thermodynamic model for the solubility of PuO_2(am) in the aqueous K^+-HCO_3^--CO_3^{2-}-OH^--H_2O system. Radiochim. Acta 86, 89–100. https://doi.org/10.1524/ract.1999.86.34.89.
Rai, D., Yui, M., Kitamura, A., 2012. Thermodynamic model for amorphous $Pd(OH)_2$ solubility in the aqueous Na^+–K^+–H^+–OH^-–Cl^-–ClO^{4-}–H_2O system at 25 °C: a critical review. J. Solut. Chem. 41, 1965–1985.
Russell, A.S., Edwards, J.D., Taylor, C.S., 1955. Solubility and density of hydrated aluminas in NaOH solutions. J. Occup. Med. 7, 1123–1128. https://doi.org/10.1007/BF03377627.
Santschi, P.H., Schindler, P.W., 1974. Complex formation in the ternary systems Ca–H_4SiO_4–H_2O and Mg–H_4SiO_4–H_2O. J. Chem. Soc. Dalton Trans. 181–184. https://doi.org/10.1039/DT9740000181.
Scatchard, George, 1936. Concentrated solutions of strong electrolytes. Chem. Rev. 19, 309–327. https://doi.org/10.1021/cr60064a008.
Schepperle, J., 2020. Löslichkeit Von Plutonium Und Neptunium in An- Und Abwesenheit Von Carbonat. Karlsruher Institut für Technologie (KIT).
Schramm, M., 2013. Mineralogisch-geochemische Nachuntersuchungen Des Kaliflözes Staßfurt Im Grubengebäude Der Schachtanlagen Bartensleben Und Marie. Bundesgesellschaft für Endlagerung (BGE).
Scribano, V., Carbone, S., Manuella, F.C., Hovland, M., Rueslåtten, H., Johnsen, H.-K., 2017. Origin of salt giants in abyssal serpentinite systems. Int. J. Earth Sci. 106, 2595–2608. https://doi.org/10.1007/s00531-017-1448-y.
Sjöberg, S., Hägglund, Y., Nordin, A., Ingri, N., 1983. Equilibrium and structural studies of Silicon(iv) and Aluminium(iii) in aqueous solution. V. Acidity constants of Silicic Acid and the ionic product of water in the medium range 0.05–2.0 M Na(CI) at 25°C. Mar. Chem. 13, 35–44. https://doi.org/10.1016/0304-4203(83)90047-6.
Solov'eva, E.F., 1946. Izvestiya Vsesoyuznogo Nauchno-issledovatel'skogo Instituta Gidrotekhniki.
Spencer, R.J., Møller, N., Weare, J.H., 1990. The prediction of mineral solubilities in natural waters: a chemical equilibrium model for the Na-K-Ca-Mg-Cl-SO_4-H_2O system at temperatures below 25°C. Geochem. Cosmochim. Acta 54, 575–590. https://doi.org/10.1016/0016-7037(90)90354-N.
StandAG, 2023. Gesetz zur Suche und Auswahl eines Standortes für ein Endlager für hochradioaktive Abfälle (Standortauswahlgesetz - standag) vom 05. Mai 2017 (Bgbl. I S. 1074), Zuletzt Geändert Durch Artikel 8 Des Gesetzes Vom 22. März 2023 (Bgbl. 2023 I Nr. 88).
Thoenen, T., Hummel, W., Berner, U., Curti, E., 2014. The PSI/Nagra Chemical Thermodynamic Database 12/07.
Turner, D.R., Achterberg, E.P., Chen, C.-T.A., Clegg, S.L., Hatje, V., Maldonado, M.T., Sander, S.G., van den Berg, C.M.G., Wells, M., 2016. Toward a quality-controlled and accessible pitzer model for seawater and related systems. Front. Mar. Sci. 3. https://doi.org/10.3389/fmars.2016.00139.
van't Hoff, J.H., Meyerhoffer, W., 1899. Über Anwendungen der Gleichgewichtslehre auf die Bildung oceanischer Salzablagerungen mit besonderer Berücksichtigung des Stassfurter Salzlagers. Zeitschrift für physikalische Chemie 30, 64–88.
Visjagin, N.I., 1939. Bull. Inst. Galurg. 10–11, 21–23.
Voigt, W., 2023. Implementation of carbonates and CO_2 into the T-dependent pitzer model of Oceanic systems. I. System NaOH – $Mg(OH)_2$ – $Ca(OH)_2$ – CO_2 – H_2O. THEREDA-Journal 03.
Voigt, W., 2020. Hexary system of Oceanic Salts – polythermal Pitzer Dataset (numerical supplement). THEREDA-Journal 1.
Wagner, T., Kulik, D.A., Hingerl, F.F., Dmytrieva, S.V., 2012. GEMSelektor geochemical modeling package: TSolMod Library and data interface for multicomponent phase models. Can. Mineral. 50, 1173–1195. https://doi.org/10.3749/canmin.50.5.1173.
Warren, J.K., 2016. Evaporites: a Geological Compendium. Springer.
Wasserdichte Verdämmung im Salzgebirge, 1902. Wasserdichte Verdämmung im Salzgebirge. Gluckauf 38, 307–309.
Wesolowski, D.J., 1992. Aluminum speciation and equilibria in aqueous solution: I. The solubility of gibbsite in the System Na-K-Cl-OH-Al$(OH)_4$ from 0 to 100°C. Geochem. Cosmochim. Acta 56, 1065–1091. https://doi.org/10.1016/0016-7037(92)90047-M.
Wolery, T., 1992. EQ3/6, a software package for geochemical modeling of aqueous systems: package overview and installation guide, Version 7.0. https://doi.org/10.2172/138894.
Wolery, T.J., Jackson, K.J., Bourcier, W.L., Bruton, C.J., Viani, B.E., Knauss, K.G., Delany, J.M., 1990. Current status of the EQ3/6 software package for geochemical modeling. In: Chemical Modeling of Aqueous Systems II, ACS Symposium Series. American Chemical Society, pp. 104–116. https://doi.org/10.1021/bk-1990-0416.ch008.
Xie, M., Kolditz, O., Moog, H.C., 2011. A geochemical transport model for thermo-hydro-chemical (THC) coupled processes with saline water. Water Resour. Res. 47. https://doi.org/10.1029/2010WR009270.
Xie, N., Dang, Y., Shi, X., 2019. New insights into how $MgCl_2$ deteriorates Portland cement concrete. Cement Concr. Res. 120, 244–255. https://doi.org/10.1016/j.cemconres.2019.03.026.
Xiong, Y., 2013. A thermodynamic model for Silica and aluminum in alkaline solutions with high ionic strength at elevated temperatures up to 100 °C: applications to zeolites. Am. Mineral. 98, 141–153. https://doi.org/10.2138/am.2013.4089.
Xiong, Y., Domski, P., 2016. Updating the WIPP Thermodynamic Database, Revision 1, Supersedes ERMS 565730. Sandia National Laboratories, Carlsbad, NM. ERMS 566047.
Xiong, Y., Kirkes, L., Marrs, C., Knox, J., 2017. Am(III)/Nd(III) interactions with Borate: experimental investigations of $Nd(OH)_3$(micro cr. Solubility in Nacl Solutions in Equilibrium with Borax.
Xu, T., Spycher, N., Sonnenthal, E., Zhang, G., Zheng, L., Pruess, K., 2011. TOUGHREACT version 2.0: a simulator for subsurface reactive transport under non-isothermal multiphase flow conditions. Comput. Geosci. 37, 763–774. https://doi.org/10.1016/j.cageo.2010.10.007.
Yalcintas, E., Cevirim-Papaioannou, N., Gaona, X., Fellhauer, D., Neck, V., Altmaier, M., 2019. Solubility of U(VI) in chloride solutions. III. The stable Oxides/Hydroxides in $MgCl_2$ systems: Pitzer activity model for the system UO_2^{2+}–Na^+–K^+–Mg^{2+}–H^+–OH^-–Cl^-–H_2O(l). J. Chem. Therm. 131, 375–386. https://doi.org/10.1016/j.jct.2018.10.019.
Yalçıntaş, E., Gaona, X., Altmaier, M., Dardenne, K., Polly, R., Geckeis, H., 2016. Thermodynamic description of tc(iv) solubility and hydrolysis in dilute to concentrated NaCl, $MgCl_2$ and $CaCl_2$ solutions. Dalton Trans. 45, 8916–8936. https://doi.org/10.1039/C6DT00973E.
Yan, Y., Çevirim-Papaioannou, N., Gaona, X., Fellhauer, D., Altmaier, M., 2024. Thermodynamic description of U(IV) solubility and hydrolysis in chloride systems: Pitzer activity model for the system U^{4+}–Na^+–Mg^{2+}–Ca^{2+}–H^+–Cl^-–OH^-–H_2O(l). Appl. Geochem. 171, 106091. https://doi.org/10.1016/j.apgeochem.2024.106091.
Yanat'eva, O.K., 1948. Equilibrium in the Sea-Water system Na, Mg||Cl, SO_4H_2O at 55°. II. Zh. Prikl. Khim. 21, 26–34.
Yang, J., Peng, J., Duan, Y., Tian, C., Ping, M., 2012. The phase diagrams and pitzer model representations for the system KCl^+ $MgCl^{2+}$ H_2O at 50 and 75°C. Russ. J. Phys. Chem. A 86, 1930–1935.